ELECTROACTIVE ION EXCHANGE MEMBRANES

BASED ON CONDUCTING POLYMERS

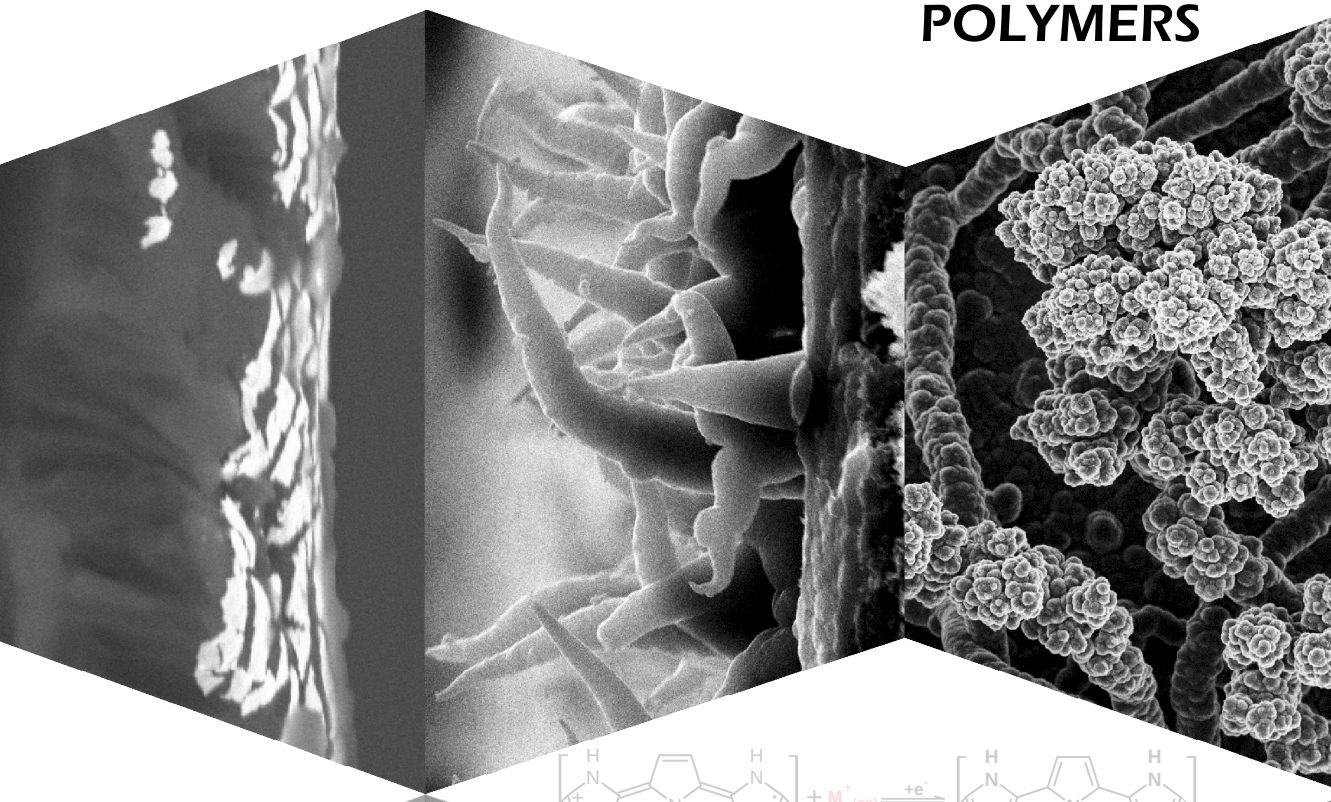

Marceline Neg Akieh-Pirkanniemi

Laboratory of Analytical Chemistry

Process Chemistry Centre

Department of Chemical Engineering

Åbo Akademi University

Åbo, Finland, 2012

Marceline Neg Akieh-Pirkanniemi

MSc in Applied Polymer Science, 2005
Martin-Luther Universität Halle-Wittenberg, Germany

PhD studies from 2008 to 2012 (maternity leave in 2011)
Åbo Akademi University, Finland

Electroactive Ion Exchange Membranes
based on conducting polymers

Marceline Neg Akieh-Pirkanniemi

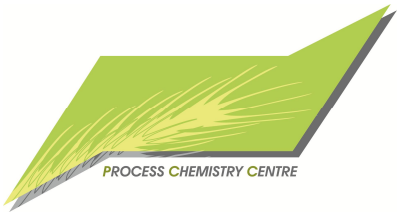

Laboratory of Analytical Chemistry
Process Chemistry Centre
Department of Chemical Engineering
Åbo Akademi University
Åbo, Finland
2012

Supervisors

Professor Ari Ivaska
Laboratory of Analytical Chemistry
Department of Chemical Engineering
Åbo Akademi University
Åbo, Finland

Docent Johan Bobacka
Laboratory of Analytical Chemistry
Department of Chemical Engineering
Åbo Akademi University
Åbo, Finland

Associate Professor Stephen Ralph
School of Chemistry
University of Wollongong
New South Wales, Australia

Reviewers

Professor Csaba Visy
Department of Physical Chemistry and Material Science
Faculty of Science and Informatics
University of Szeged
Szeged, Hungary

Professor Leif Nyholm
Ångström Laboratory, Analytical Chemistry
Department of Chemistry
University of Uppsala
Uppsala, Sweden

Opponent

Professor Csaba Visy
Department of Physical Chemistry and Material Science
Faculty of Science and Informatics
University of Szeged
Szeged, Hungary

ISBN 978-952-12-2820-9
Painosalama Oy – Turku, Finland 2012

To my Mammy and Papa, who didn't wait to enjoy the fruit of their labour

Preface

The work presented in this thesis was mainly carried out in the Laboratory of Analytical Chemistry, Åbo Akademi University from September 2008 to December 2012 (During this period the author was on Maternity leave from March 2011 to January 2012). The Laboratory of Analytical Chemistry belongs to the Process Chemistry Centre, which was appointed as a Centre of Excellence in Research by the Academy of Finland from 2000 – 2011 and continues with other funding sources. A personal scholarship to pursue the PhD studies from the Magnus Ehrnrooth Foundation for a period of 2 years is gratefully acknowledged. The Graduate School of Chemical Engineering (GSCE) and PCC are acknowledged for financing the rest of the studies. In addition, I would like to thank Åbo Akademi Foundation, GSCE and the Rector of Åbo Akademi University for financially supporting my conference trips.

A journey of miles begins with a step. The first step took me to Australia where I met Associate Professor Stephen Ralph and Professor William Price. Their constant support, advice and encouragement during my four months stay in the University of Wollongong will forever be cherished. There I got acquainted with polypyrrole. Though from a distance, Steve has been a constant guide throughout my PhD studies. I am grateful to his patience and his fruitful comments in contribution to the success of all our publications together. Call it faith or luck but whatever it is, I am glad I ended up at the door step of the Laboratory of Analytical Chemistry. It has been an honour and a pleasure to work with Professor Johan Bobacka and Professor Ari Ivaska. Thank you for always keeping your doors open and for never being tired of my endless questions. You are the best supervisors a student can ever ask for and the best reviewers a writer can have. Thank you for teaching me and for nurturing me into the scientist I have become.

I would like to thank all my co-authors for all their valuable contributions to all my publications, especially Kevin Vavra, who performed part of the experiments in Paper V. Special thanks go to Dr. Rose-Marie Latonen for always being there for me in case of any help relating to my thesis and research in general. Thank you also for reading and commenting on the first draft of my thesis. I would also like to thank Mr. Luis Bezerra for training me on how to use the ion chromatography and Dr. Tiina Saloranta for providing distilled pyrrole at the very beginning of my research. My sincere gratitude

goes to our very own trio in the group: Sten, Paul and Lassi. Thank you, Sten, for helping out with all the practical arrangements in the Laboratory and with the ICP measurements. Thanks to Lassi and Paul for helping with designing and building the cells and accessories used in my experiments. It has been a great pleasure to work with you my amazing and dear colleagues. For such a small unit, it has one of the most international atmospheres you can find, from which I have learnt a lot. I appreciate all the help I have received. It has not been easy being a mother, a wife and a researcher. Thank you for a friendly and warm working environment and *'Xie Xie'* to my office room-mates. I would also like to acknowledge Ulriika and Ari for helping out in translating the abstract into Swedish and Finnish.

I am grateful to Professor Csaba Visy and Professor Leif Nyholm for reviewing my thesis and for the helpful comments suggested in improving the thesis. I will also like to acknowledge Prof. Csaba Visy for accepting to be the opponent of my PhD defence.

I would like to say thank you to all my dear friends, with whom I have been together right from the beginning, especially Bri, Katja and Valerie who understand the tedious business of PhD and family. Thank you for your support and being such great friends. Being in Finland all these years, I have come to surround myself with very special people. This PhD would never have been completed in due time without the support, help, and encouragement and not forgetting babysitting from Maija, Eli, Valerie, Tere and Janne. *Merci à Iderline, Floriane et Mariette pour l'aide que vous m'avez apportée particulierement pour s'être occupé de mes enfants quand j'avais du travail à l'université.* Thank you my fellow Cameroonians in Turku (CAMTU ry) for the joyful times together and for your support.

Haluan kiittää perhettäni Suomessa. Olen kiitollinen, että minulla on teidänlaisenne appivanhemmat. Kohtelette minua kuin omaa lastanne, mitä tulen aina arvostamaan. Kiitos myös väitöstutkimustani kohtaan esittämästänne kiinnostuksesta ja siitä, miten huolehditte lapsistani.

My profound gratitude goes to my dear brothers and sisters who have always been there for me. Your everlasting trust, love, support and encouragement mean the world to me. Thank you for believing in me and for always keeping me on track. Family is very important to me and I am grateful that we are always there for one another. In the heat of the moment we turn to each other and we know that we have each other's back. What

a pity my parents are not able to witness this. My Father was a believer in education, he believed in me even when I did not believe in myself.

My everlasting gratitude is reserved to the love of my life, my darling husband. You have been very helpful and supportive throughout my PhD studies. You have always been the first to read my manuscript and my thesis, and for that I say thank you. We have achieved a lot in such a short time together. Thanks for taking care of the children while I am working, studying or relaxing after a tiring day at the university. You are the best Dad in the world, our children are very lucky. My heart goes to my marvellous children, who are special and unique. To my darling Elle (the greatest big sister), my sweet Karita and my sunshine Leo …thank you for being such cute kids.

In Åbo, on a peaceful and dark day in November 2012,

Abstract

Ion exchange membranes are indispensable for the separation of ionic species. They can discriminate between anions and cations depending on the type of fixed ionic group present in the membrane. These conventional ion exchange membranes (CIX) have exceptional ionic conductivity, which is advantageous in various electromembrane separation processes such as electrodialysis, electrodeionisation and electrochemical ion exchange. The main disadvantage of CIX membranes is their high electrical resistance owing to the fact that the membranes are electronically non conductive. An alternative can be electroactive ion exchange membranes, which are ionically and electronically conducting. Polypyrrole (PPy) is a type of electroactive ion exchange material as well as a commonly known conducting polymer. When PPy membranes are repeatedly reduced and oxidised, ions are pumped through the membrane.

The main aim of this thesis was to develop electroactive cation transport membranes based on PPy for the selective transport of divalent cations. Membranes developed composed of PPy films deposited on commercially available support materials. To carry out this study, cation exchange membranes based on PPy doped with immobile anions were prepared. Two types of dopant anions known to interact with divalent metal ions were considered, namely 4-sulphonic calix[6]arene (C6S) and carboxylated multi-walled carbon nanotubes (CNT). The transport of ions across membranes containing PPy doped with polystyrene sulphonate (PSS) and PPy doped with para-toluene sulphonate (pTS) was also studied in order to understand the nature of ion transport and permeability across PPy(CNT) and PPy(C6S) membranes. In the course of these studies, membrane characterisation was performed using electrochemical quartz crystal microbalance (EQCM) and scanning electron microscopy (SEM). Permeability of the membranes towards divalent cations was explored using a two compartment transport cell.

EQCM results demonstrated that the ion exchange behaviour of polypyrrole is dependent on a number of factors including the type of dopant anion present, the type of ions present in the surrounding medium, the scan rate used during the experiment and the previous history of the polymer film. The morphology of PPy films was found to change when the dopant anion was varied and even when the thickness of the film was altered in some cases. In nearly all cases the permeability of the membranes towards

metal ions followed the order $K^+ > Ca^{2+} > Mn^{2+}$. The one exception was PPy(C6S), for which the permeability followed the order $Ca^{2+} \geq K^+ > Mn^{2+} > Co^{2+} > Cr^{3+}$. The above permeability sequences show a strong dependence on the size of the metal ions with metal ions having the smallest hydrated radii exhibiting the highest flux. Another factor that affected the permeability towards metal ions was the thickness of the PPy films. Films with the least thickness showed higher metal ion fluxes. Electrochemical control over ion transport across PPy(CNT) membrane was obtained when films composed of the latter were deposited on track-etched Nucleopore® membranes as support material. In contrast, the flux of ions across the same film was concentration gradient dependent when the polymer was deposited on polyvinylidene difluoride membranes as support material. However, electrochemical control over metal ion transport was achieved with a bilayer type of PPy film consisting of PPy(pTS)/PPy(CNT), irrespective of the type of support material.

In the course of studying macroscopic charge balance during transport experiments performed using a two compartment transport cell, it was observed that PPy films were non-permselective. A clear correlation between the change in pH in the receiving solution and the ions transported across the membrane was observed. A decrease in solution pH was detected when the polymer membrane acted primarily as an anion exchanger, while an increase in pH occurred when it functioned as a cation exchanger. When there was an approximately equal flux of anions and cations across the polymer membrane, the pH in the receiving solution was in the range 6 - 8. These observations suggest that macroscopic charge balance during the transport of cations and anions across polypyrrole membranes was maintained by introduction of anions (OH^-) and cations (H^+) produced via electrolysis of water.

Referat

Jonbytesmembraner har stor betydelse vid separering av joniska komponenter. Dessa membraner kan antingen byta ut anjoner eller katjoner beroende av den jonbytande gruppens kemiska egenskaper. De konventionella jonbytesmembranerna (CIX) har jonisk ledningsförmåga som kan utnyttjas med förmån vid olika separationsprocesser såsom elektrodialys, elektrodejonisation och elektrokemiskt jonbyte. Den största nackdelen med CIX-membraner är att de är isolatorer och sahnar elektronisk ledningsförmåga. Ett alternativ till CIX-membraner som jonbytande material är elektroaktiva polymerer som har både elektroniskt och jonisk ledningsförmåga. Polypyrrol (PPy) som är en av de mest använda elektriskt ledande polymererna har också jonbytesegenskaper. Då en membran av PPy kontinuerligt reduceras och oxideras kommer joner att transporteras genom den.

Målet med detta arbete var att utveckla elektroaktiva jonbytesmembraner av PPy för selektiv överföring av katjoner mellan två lösningar. För detta ändamål syntetiserades katjonbytande membraner av PPy dopade med immobila anjoner. Två typer av anjoner användes: 4-sulfoncalix[6]aren (C6S) och karboxylerade ”multi-walled” kolnanotuber (CNT). PPy-membraner dopade med polystyrensulfonat (PPS) och para-toluen sulfonat (pTS) anjoner undersöktes också för att klargöra jontransportmekanismen genom PPy(CNT)- och PPy(C6S)-membraner. Elektrokemisk kvartskristallmikrovåg (EQCM) och svep elektromikroskop (SEM) användes för karakterisering av de undersökta materialen. Membranernas permeabilitet för mono-och divalenta joner undersöktes i en special cell där den undersökta membranen separerade två lösningar mellan vilka jontransporten skedde.

På basen av EQCM-resultaten kunde man dra den slutsatsen att jonöver-föringsegenskaperna av PPy beror på flera faktorer: dopande anjonen, vilka andra joner det finns i lösningen, potentialens svephastighet och för vilka fysikaliska och kemiska påfrestningar filmen hade varit utsatt före experimentet. PPy-filmens morfologi förändrades då dopningsjonen byttes och även i vissa fall då filmtjockleken varierades. I nästan alla undersökta fall erhölls följade ordning för de undersökta metalljonernas permeabilitet: $K^+ > Ca^{2+} > Mn^{2+}$. Undantaget var PPy(C6S)-membranen för vilken ordningen var: $Ca^{2+} \geq K^+ > Mn^{2+} > Co^{2+} > Cr^{3+}$. De funna permeabilitetsordningarna visar ett starkt beroende av jonstorleken och att metalljoner med den minsta jonradien

har den högsta permeabiliteten. PPy-membranens tjocklek är också en avgörande faktor för jontransport genom membranen. Tunna membraner visade hög permeabilitet. Då tjockleken ökade blev membranerna också mera selektiva samtidigt som jontransporten minskade. Jonöverföring genom PPy(CNT)-membranen kunde kontrolleras elektrokemiskt då den hade placerats på en ”track-etched” Nucleopore®-membran som fungerade som stödmaterial. Då jonbytesmembranen var placerad på en porös polyvinylendifluorid blev jontransporten beroende endast av koncentrationsgradienten mellan lösningarna. Men då man använde membraner som bestod av två lager av olikt dopade filmer, PPy(pTS)/PPy(CNT) kunde jontransporten kontrolleras elektrokemist oberoende av stödmembranets material.

Då man studerade den makroskopiska laddningsbalansen i den använda special cellen upptäckte man en tydlig korrelation mellan förändringen i pH i den mottagande lösningen och de joner som transporterades genom membranen. Den mottagande lösningens pH sjönk då membranen fungerade som anjonbytare och ökning i pH observerades då membranen fungerade som katjonbytare. Då både an- och katjoner transporterades genom membranen hölls pH i den mottagande lösningen neutral, d.v.s. 6 – 8. Dessa resultat tyder på att den makroskopiska laddningsbalansen erhölls genom bildning av väte- och hydroxidjoner vid vattnets elektrolys i den mottagande lösningen.

List of Publications

This thesis is a summary of the publications listed below, which are also referred to in the text by their Roman numerals. The original publications are included as re-prints with copyright permission.

I. Marceline N. Akieh, William E. Price, Johan Bobacka, Ari Ivaska, Stephen F. Ralph. *Ion exchange behaviour and charge compensation mechanism of polypyrrole in electrolytes containing mono-, di- and trivalent metal ions.* **Synthetic Metals** 159 (2009) 2590–2598.

II. Marceline N. Akieh, Stephen F. Ralph, Johan Bobacka, Ari Ivaska. *Transport of metal ions across an electrically switchable cation exchange membrane based on polypyrrole doped with a sulfonated calix[6]arene.* **Journal of Membrane Science** 354 (2010) 162–170.

III. Marceline N. Akieh, Ágnes Varga, Rose-Marie Latonen, Stephen F. Ralph, Johan Bobacka, Ari Ivaska. *Simultaneous monitoring of the transport of anions and cations across polypyrrole based composite membranes.* **Electrochimica Acta** 56 (2011) 3507–3515.

IV. Marceline N. Akieh, Rose-Marie Latonen, Sten Lindholm, Stephen F. Ralph, Johan Bobacka, Ari Ivaska. *Electrochemically controlled ion transport across polypyrrole/multi-walled carbon nanotube composite membranes.* **Synthetic Metals** 161 (2011) 1906– 1914.

V. Rose-Marie Latonen, Marceline N. Akieh, Kevin Vavra, Johan Bobacka, Ari Ivaska. *Ion exchange behavior of polypyrrole doped with large anions in electrolytes containing mono- and divalent metal ions.* **Submitted to Electroanalysis (2012).**

Author's Contribution

Papers I – IV: All experiments were planned and conducted by the author, except SEM and ICP measurements. Sample preparations for the latter analyses and data interpretation were carried out by the author. The author wrote the first draft of the manuscript and finalised it together with the co-authors. For *Paper V*, all experiments were planned by the author and performed together with one of the co-authors (except SEM and EDX analyses). The first draft of the manuscript was written by one of the co-authors and finalised by the others.

Other publications not included in the thesis

VI. Marceline N. Akieh, Manu Lahtinen, Ari Väisänen, Mika Sillanpää. *Preparation and characterization of sodium iron titanate ion exchanger and its application in heavy metal removal from waste waters.* **Journal of Hazardous Materials** 152 (2008) 640–647.

VII. Marceline N. Akieh, Manu Lahtinen, Sirpa Peräniemi, Mika Sillanpää. *The Effect of Interferences on the Uptake of Heavy Metals by Sodium (iron) Titanates from Waste Water.* **Journal of Ion Exchange** 18, 4 (2007) 334-229.

Table of Contents

Abbreviations and Symbols

a_i	activity of target ion
AXM	anion exchange membrane
A	area of working electrode
BCS	bathocuproinedisulphonic acid
C6S	4-sulphonic calix[6]arene
CDS	sulphated cyclodextrin
C_f	sensitivity factor of the crystal
CIX	conventional ion exchange membrane
CNT	carboxylated multi-walled carbon nanotubes
CP	conducting polymer
CV	cyclic voltammetry
CXM	cation exchange membrane
DBS	dodecylbenzene sulphonate
e^-	electron
E^0	standard potential
EaIX	electroactive ion exchange
ED	electrodialysis
EDI	electrodeionisation
EDXA	energy dispersive X-ray analysis
EIX	electrochemical ion exchange
EQCM	electrochemical quartz crystal microbalance
ESCR	electrochemically stimulated conformational relaxation
ESP	electrostatic precipitator
F	Faraday constant
f_0	resonance frequency
HQS	8-hydroxyquinoline-5-sulphonic acid
IC	ion chromatography
ICP-OES	inductively coupled plasma-optical emission spectroscopy
ISE	ion selective electrode
ISM	ion selective membrane
M'	apparent molar mass
N	number of moles of electrolysed material
NiHCF	nickel hexacyanoferrate
PA	polyacetylene

PC	Nucleopore® track-etched polycarbonate
PLED	polymer light emitting diode
PPP	polyparaphenylene
PPy	polypyrrole
PPy(BCS)	polypyrrole doped with bathocuproinedisulphonate
PPy(Cl)	polypyrrole doped with chloride
PPy(HQS)	polypyrrole doped with 8 hydroxyquinoline-5-sulphonate
PPy(C6S)	polypyrrole doped with 4-sulphonic calix[6]arene
PPy(α-CDS)	polypyrrole doped with sulphated α-cyclodextrin
PPy(β-CDS)	polypyrrole doped with sulphated β-cyclodextrin
PPy(ClO_4)	polypyrrole doped with perchlorate
PPy(CNT)	polypyrrole doped with carboxylated multi-walled carbon nanotubes
PPy(PSS)	polypyrrole doped with polystyrene sulphonate
PPy(pTS)	polypyrrole doped with para-toluene sulphonate
PSS	polystyrene sulphonate
PT	polythiophene
pTS	para-toluene sulphonate
PVDF	polyvinylidene difluoride
PVS	polyvinylsulphate
Q	charge
R	universal gas constant
SEM	scanning electron microscopy
μ_q	shear modulus of the crystal
SHE	standard hydrogen electrode
T	absolute temperature
z	charge on the transferred ion
z_i	charge of the target ion
α	separation/selectivity factor
Δf	change in frequency
Δm	mass change per unit area
ρ_q	density of the crystal
n	overtone number

1. Introduction

The growing interest in membrane technology is overwhelming especially in industrial sectors such as biotechnology, nanotechnology, energy storage devices and purification and separation technologies. When compared to other processes, membrane technologies provide clean and energy efficient methods in solute recovery and solvent purification. Membrane technology is employed in a wide range of processes, in which the membranes are developed to meet the demands required by the process. Processes involving the use of membranes include reverse osmosis, nanofiltration, ultrafiltration, microfiltration, fuel cells, sensors, and electromembrane processes. Ion exchange membranes are of commercial interest, but less important than other membranes used in processes such as reverse osmosis, nanofiltration and ultrafiltration. Nonetheless for the separation of ionic species, ion exchange membranes are without competition. Ion exchange membranes can discriminate between cations and anions, and in specific cases they can be made to be monovalent ion selective [1-4] or even proton selective [5,6]. The commercialisation of ion exchange membranes was achieved some 50 years ago. These early membranes were thin sheets of material containing fine ion exchange resins held together by binders. Later on, rather complex ion exchange membranes were developed with properties tailored for specific applications e.g. mosaic membranes and bipolar membranes. Ion exchange membranes have exceptional ionic conductivity, which is advantageous in electromembrane processes [7]. The properties of a good ion exchange membrane are high ion permselectivity, low electric resistance, low rate of electro-osmosis for high solution concentration, and good chemical, mechanical and physical stability [8]. These requirements always have conflicting effects on each other and on the properties of the membrane. An example of such an opposing effect is explained by considering electrical resistance. A membrane that has low electrical resistance should be thin with a high ion exchange capacity. However, a high ion exchange capacity increases the swelling of the membrane, which in turns decreases the content of fixed ions and also the physical durability of the membrane [8]. Thus, a compromise must be reached by the manufacturer, where all the parameters are carefully considered in order to develop an ion exchange membrane to be utilised in one of the numerous electromembrane processes.

Conventional ion exchange (CIX) membranes may in the future be replaced by a novel type of material, electroactive ion exchange (EaIX) membranes. Conventional ion exchangers are good ionic conductors because of the mobility of their exchangeable ions, however, they posses no electronic conductivity [9]. One of the main problems in dealing with CIX membranes is high electrical resistance, which determines the energy required by the electrodialysis process [10]. EaIX membranes, on the other hand, are good ionic and electronic conductors. In regards to conflicts between different membrane properties, electroactive ion exchange polymers are advantageous especially because their electrical resistance is low. The ion exchange capacities of EaIX can be changed by electrochemical or chemical means. Some types of EaIX (e.g. conducting polymers, CPs) can be switched from an anion to a cation exchanger [9]. The rate of ion exchange for CPs is lower than for conventional ion exchange resins. This is because CPs have a compact nature mainly arising from interchain interactions, and interactions between the charged polymer backbone and mobile ions [9]. Nonetheless, the ion exchange capacity of a CP (e.g. polypyrrole doped with chloride)) is reported to be equivalent to that of conventional ion exchange resins and membranes [11].

EaIX processes involve ion uptake and elution by modulating the potential of an ion exchange film [12]. The ion exchange medium is an electroactive ion exchange material. Generally, the process involving cation uptake and release with a cation electroactive exchange material is expressed in Reaction 1 (R1). When a negative potential is applied to the ion exchange material, the electroactive material becomes reduced and cations from the surrounding electrolyte must be intercalated to maintain charge balance. When a positive potential is applied, the electroactive material becomes reoxidised and cations are eluted back into the surrounding electrolyte, in order to maintain charge neutrality. For anion exchange processes, uptake and elution of ions are initiated by oxidation and reduction of the anion exchange electroactive material (Reaction 2, R2). Reactions 1 and 2 are general reactions for a material that can be reduced and oxidised. However, for specific electroactive materials e.g. conducting polymers, R1 is valid for n-type conducting polymers while R2 is valid for p-type conducting polymers. The ability of conducting polymers to act electroactive ion exchange materials is fully described in sections 3 and 4 of this thesis. Reaction 3 (R3) involves exchange of ions without necessarily removing from or adding electrons to a material. This third process in which

ions of higher affinity are exchanged for ions of lower affinity is similar to conventional ion exchange processes.

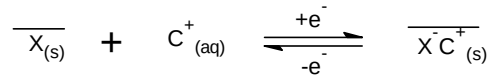

R1

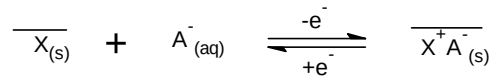

R2

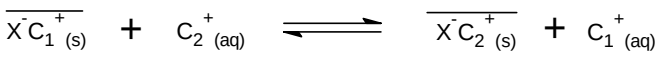

R3

Where, $\overline{X_{(s)}}$ is an electroactive ion exchanger, C^+ is a univalent cation, A^- is a univalent anion.

As already mentioned EaIX involves absorption and desorption of ions through redox reactions of the ion exchange material. Thus, this method does not require additional chemicals (acid or base) for regeneration and as a result there is a significant decrease in secondary waste production [12]. Secondary waste production is one of the major disadvantages in dealing with conventional ion exchange resins. Research on electroactive ion exchange membrane is still only carried out on the laboratory scale. To the author's knowledge, there is no industrial application of this process yet. This is partly because of the challenges faced in producing membranes with large surface areas at low cost [13]. Despite its huge potential, EaIX is a relatively new area of research with the first studies carried out only some 30 years ago [14]. In order for this approach to be fully utilised on a large scale, further work needs to be performed. In this thesis some of the issues arising concerning selectivity, stability, ion exchange and transport mechanism, and exploitation of different electroactive ion exchange materials are tackled.

2. Ion Exchange Membranes

Ion exchange membranes are thin sheets of polymeric material containing fixed ionic groups. Depending on the type of ionic group, they are classified as cation or anion exchange membranes. Cation exchange membranes contain fixed negatively charged groups e.g. SO_3^-, COO^-, PO_3^{2-} and PO_3H^- which allow the transport of cations and result in rejection of anions. Anion exchange membranes have fixed positively charged groups e.g. NH_3^+, NRH_2^+, NR_2H^+, and NR_3^+, which allow the transport of anions but reject cation [15]. Ion exchange membranes can also be distinguished as homogenous or heterogeneous according to their chemical homogeneity [15-17]. Heterogeneous membranes have at least two phases and can be prepared from a mixture of ion exchange resins and a polymer binder. Homogenous ion exchange membranes have only one phase where a single polymer provides structural strength and functions as the ion exchange matrix [17]. Ion exchange membranes are widely used in electrodialysis, e.g. for demineralisation/desalination and concentrating electrolyte solutions (salt production) [6]. The development of Nafion® by DuPont led to the application of cation exchange membranes for use in chlor-alkali production and in fuel cell production [18]. The development of new ion exchange membranes with improved properties (selectivity, electrical resistance, and thermal, chemical and mechanical robustness) opened new doors for applications in other sectors such as the food, drug and chemical process industries, and wastewater treatment [19, 20]. Examples of processes which utilise ion exchange membranes are described briefly in the next section.

2.1. Conventional Ion Exchange Membrane Processes

2.1.1. Electrodialysis

In electrodialysis (ED), ions are transported across ion exchange membranes under the influence of an applied electric field with the intention of separating anions and cations. The process takes place in an electrodialysis cell, where an alternating series of anion and cation exchange membranes are placed between two electrodes (anode and cathode) [17]. Figure 1 shows a single cell of an electrodialysis unit with feed solution flowing through the cell. When an electric field is applied between the electrodes, cations from the feed solution migrate towards the cathode while anions migrate towards the anode. The anion (AXM) and cation exchange membranes (CXM) in the cell provide selective

transport of only anions and cations, respectively. This results in a solution of low salt concentration (diluate), in between the membranes and a solution of high salt concentration (concentrate) outside the ion exchange membranes.

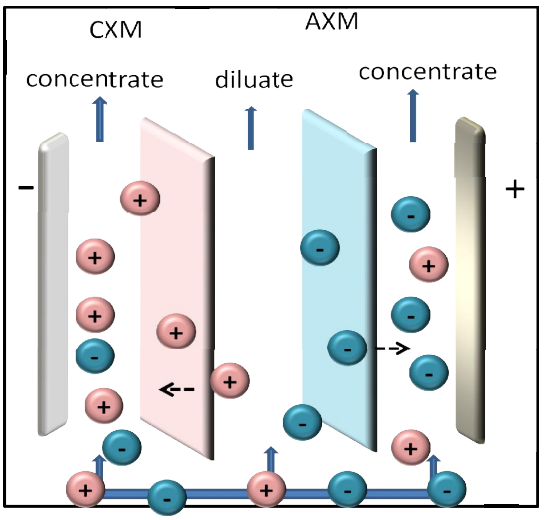

Figure 1: *Schematic illustration of a single cell unit in an electrodialysis process. CXM is a cation exchange membrane and AXM is an anion exchange membrane.*

2.1.2. Electrodeionisation

Electrodeionisation (EDI) is a separation technology that combines ion exchange and electrolysis. One of its common uses is in the production of ultrapure deionised water. In EDI a mixed bed ion exchange resin is placed into a purifying compartment between a CXM and an AXM of a conventional electrodialysis cell (Figure 2). The function of the ion exchange resin is to retain ions. Under the influence of a strong direct current applied between the anode and cathode, ions migrate towards the respective, oppositely-charged electrodes. In this way anions and cations are continuously removed and transferred into the adjacent concentrating compartments. AXM allows the transport of anions and blocks the passage of cations, while CXM allows the transport of cations and blocks the passage of anions. The strong applied electrical potential splits water generating H^+ and OH^- ions for continuous regeneration of the ion exchange resin [21, 22]. The advantage of this process is the lack of chemicals required for regeneration. However, there is inefficient usage of current [23].

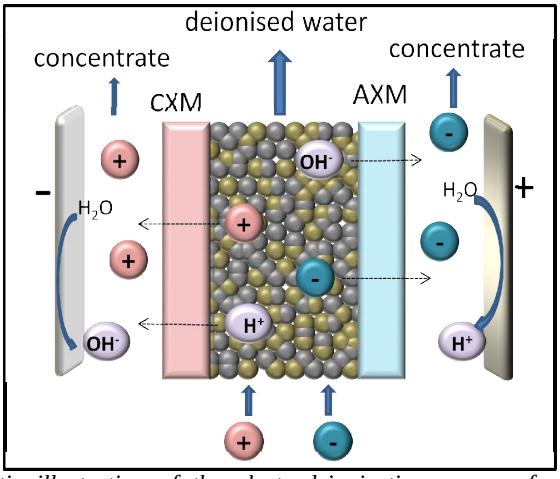

Figure 2: *Schematic illustration of the electrodeionisation process for the production of ultrapure water. CXM is a cation exchange membrane and AXM is an anion exchange membrane.*

2.1.3. Electrochemical Ion Exchange

In electrochemical ion exchange (EIX), the ion exchange material is attached directly on the surface of an electrode or integrated into a membrane structure. Heterogeneous membranes measuring between 2 and 20 mm thick are typically used, and the ion exchange materials are held together with a binder. An externally applied electric field is used to control ion uptake and elution depending on the direction of current flow. In EIX, two concomitant processes take place, the electrolysis of water at the external electrodes and ion migration through the ion exchange material. Application of a negative potential to the electrode results in the production of OH^- by the electrolysis of water, which simultaneously activates the ion exchange material to enable the uptake of cations, provided the electrode assembly harbours a cation exchange material. To elute the cation, a positive potential is applied and H^+ ions, which are required to regenerate the ion exchange material, are generated from water splitting reactions. The close proximity of the generated H^+ and OH^- to the ion exchange sites decreases the time required for uptake and elution of ions thus increasing the rate of the ion exchange process [24]. The EIX process was originally developed by AEA Technology plc (United Kingdom Atomic Energy Authority) for the treatment of low level radioactive waste [25]. Currently it is also used in treating non-nuclear waste streams for the recovery of toxic and precious metals. An EIX system is shown schematically in Figure 3, where cation exchange occurs on a high surface area macroporous cation exchange structure sandwiched between two CXMs. Adsorption of cation on the surface

of the ion exchange material occurs after an application of a negative potential. Electrochemical elution is accomplished by H^+ generated from the electrolytic splitting of water and migration of the released cations to the cathodic compartment.

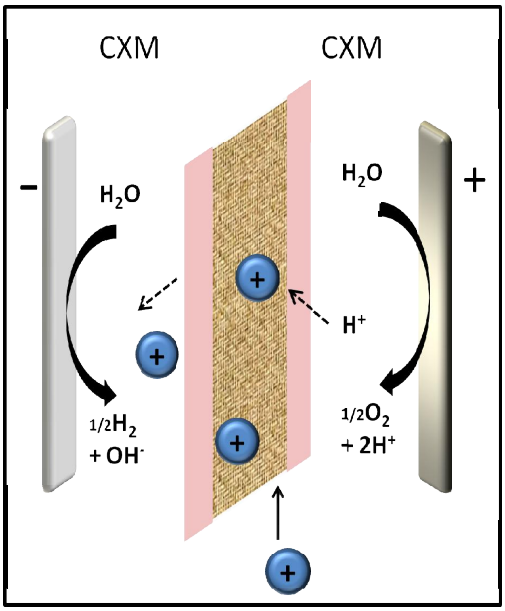

Figure 3: *Schematic illustration of the electrochemical ion exchange process. CXM is a cation exchange membrane.*

2.2. Electroactive Ion Exchange

Electroactive ion exchange (EaIX) is a novel process in which ion transport across a membrane is initiated by in situ switching of the oxidation states of the ion exchange material. It is different from the above mentioned processes in that the ion exchange membrane is both an electronic and ionic conductor. In addition, the separation mechanism for EaIX is different from conventional ion exchange membranes. Separation in an EaIX membrane is initiated by application of an electrical potential, while for conventional membranes separation is driven by differences in ionic affinity between the compounds being separated [26]. The change in pH of the solution is not a requirement for EaIX as is the case for EIX. The driving force for ion transport in EaIX is the presence of a concentration gradient and the oxidation state of the ion exchange material. This method is more energy efficient than the other above mentioned processes because it requires an applied potential typically less than 2 V. Furthermore, for CIX membranes processes e.g. EIX, electrolysis of water is required to activate and

deactivate the ion exchange sites in order to initiate transport of ions. In contrast, the transport of ions across EaIX membranes is carried out by consecutively reducing and oxidising the electroactive ion exchange material. The main criterion for such a material is electroactivity, i.e. materials that can undergo reversible oxidation and reduction. The types of materials that are suitable to be used in EaIX processes have a redox couple in which the oxidation state can be changed by application of an external potential [27].

3. Electroactive Ion Exchange Materials

Electroactive ion exchange materials can be organic or inorganic based materials that satisfy the following conditions: electronic conductivity, ionic conductivity, selectivity, and stability [12]. Two types of materials that will be discussed in this thesis have been cited in the literature as cation electroactive materials. Anion electroactive materials will not be discussed here, since the thesis is focused mainly on cation transport. A comprehensive literature is available concerning nickel hexacyanoferrates as electroactive ion exchange materials, which will be summarised in the next sub-section. A more detailed discussion will then be provided on conducting polymers, since they are the main electroactive materials studied in this thesis.

3.1. Nickel Hexacyanoferrates

Nickel hexacyanoferrates (NiHCFs), $Ni^{II}Fe^{II/III}(CN)_6^{2-/-}$, and other transition metal hexacyanoferrates are a member of the family of Prussian blue, iron(III) hexacyanoferrate(II), polynuclear compounds [28]. They are zeolite-like in structure, with an open cubic framework with channels measuring 0.32 nm in diameter. The size of the channels enables small ions to fit into the structure, but it is unable to accommodate bigger ions. Thus, smaller hydrated cations such as K^+, Rb^+, Cs^+ and NH_4^+ can be separated from bigger hydrated ions such as Na^+, Li^+ and alkaline earth metal ions [28]. Hexacyanoferrates are well known conventional ion exchangers used for the removal of Cs^+ from waste streams, due to their strong affinity for this metal ion. However, the strong affinity of these materials for Cs^+ makes regeneration after use a challenge. This led to the exploitation of alternative methods for Cs^+ decontamination. The Pacific Northwest National Laboratory (PNNL) developed an electrically switched ion exchange technique based on NiHCF films deposited on high surface area electrodes for the selective removal of Cs-137 from concentrated nuclear waste streams that also contained Na^+ and K^+ [29-35]. NiHCF is an electroactive material, which exhibits a well-defined one electron reversible redox couple in aqueous solutions containing alkali metal ions [36]. This is due to the Fe(II) centre being readily oxidised to Fe(III), and reduced back to Fe(II). During electrochemical reduction of the Fe(III) centre to the ferrous state, cations move into the film whilst during oxidation to the ferric form cations move out of the film. The driving force for the movement of cations

in and out of the film is maintenance of charge neutrality. The reduction and oxidation processes of NiHCF in the presence of Cs^+ are shown in Reaction 4 (R4).

$$NaNi^{II}Fe^{III}(CN)_6 + Cs^+ \underset{-e^-}{\overset{+e^-}{\rightleftharpoons}} NaCsNi^{II}Fe^{II}(CN)_6 \qquad R4$$

The affinity of NiHCF for alkali metal ions follows the order $Cs^+ >> K^+ > Na^+$. Thus, NiHCF can be used simultaneously as an electroactive ion exchange material and a conventional ion exchanger (Reaction 5, R5).

$$NaNi^{II}Fe^{III}(CN)_6 + 2Cs^+ \underset{-e^-}{\overset{+e^-}{\rightleftharpoons}} Cs_2Ni^{II}Fe^{II}(CN)_6 + Na^+ \qquad R5$$

Advantages of NiHCF as an electroactive ion exchange film over conventional ion exchangers (commercially available Cs-100 ion exchanger) for Cs removal from nuclear waste streams are as follows [29]:

- Cs^+ can be eluted into the same elution stream over many load cycles (1500 cycles) whereas Cs-100 is mostly able to be used once before discarded as another form of secondary waste.
- About 5 column volumes of 8 M nitric acid are needed for the effective removal of Cs^+ from the conventional ion exchanger, whereas in the EaIX process regeneration is carried out by switching the potential of the film to the reoxidised state.
- The ratio of the volume of generated secondary waste to the volume of processed waste is estimated to be two orders of magnitude lower than for a conventional ion exchange process.

Another application for NiHCF as an electroactive ion exchange material is the selective separation of K^+ from Na^+ in pulp mill streams. The separation factor (α), defined as the ratio of the mole fraction of cations in the film divided by the ratio of the mole fraction of cations in the bulk solution, indicates the selectivity for the ion of interest. The separation factor for K^+ over Na^+ for NiHCF is 24, which is higher than that of a commercially available cation exchange membrane (α = 2) [37]. In addition, NiHCF films have shown to be stable after 1500 cycles in a solution of electrostatic precipitator (ESP) catch. A hybrid system consisting of NiHCF as an electroactive ion exchange film for selective removal for K^+, and a commercial anion exchange membrane for selective separation of Cl^-, has been developed to enhance water recycling opportunities in pulp mills [37].

3.2. Conducting Polymers

Conducting polymers (CPs) are organic polymers that conduct electricity. The polymer structure consists of alternating single (σ-bonds) and double (π-bonds) bonds. These materials are also known as conjugated polymers. Conduction of electricity is an intrinsic property of these polymers where the electrons in the σ-bonds are fixed holding the carbon atoms together while electrons in the π-bonds are mobile and can be relatively easily removed or added in order to form a polymeric ion [38]. The differences between conjugated polymers and conventional polymers are noted as follows [39]:

1) The electronic band gaps in conducting polymers are relatively small (1 – 4 eV).
2) The polymer chain in a conducting polymer can be easily oxidised or reduced to form polymeric ions, in which charge neutralisation can be achieved through the incorporation or expulsion of other ions.
3) The mobility of charge carriers is high enough in CPs so that these polymers can be highly conductive in their doped state.
4) The charge carriers in CPs are not free electrons or holes but quasi particles (e.g. solitons, polarons and bipolarons).

The intrinsic conductivity displayed by these types of polymers has led to other names such as intrinsically/inherently conducting polymers. This property separates them from other types of polymers that can also conduct electricity, such as composites consisting of conventional polymers loaded with conductive filler (e.g. metal), and redox polymers [40,41].

CPs possess a unique blend of properties including, processability and electrical conductivity. Another feature of CPs is their electroactivity, which is the ability to undergo reversible changes between two or more oxidation states. This is a very important characteristic of CPs, as it provides a mechanism by which their chemical and physical properties, such as colour, volume, porosity, and electrical conductivity, can be altered by electrochemical means. Due to these properties CP materials can be produced which are capable of allowing the movement of anions, cations and neutral species in and out of the material while simultaneously changing the conductivity and redox properties of the polymer. The diversity in properties displayed by CPs has led to the use of these materials in many technical applications e.g. sensors, actuators, solar cells,

polymer light emitting diodes (PLED), membranes [13,42] and energy storage devices [43-45]. In the case of applications as electroactive ion exchangers, it is the conductivity and electroactivity that is taken advantage of. The ability of conducting polymers to act as an electroactive ion exchange material is a consequence of the changes in oxidation state and simultaneous movement of ions in and out of the polymer when an electric potential is applied.

3.2.1. Classification of Conducting Polymers

CPs can be classified as degenerate or non degenerate according to their charge transfer mechanism. Polyacetylene (PA) is an example of a CP that has a degenerate ground state. This means that its two geometric resonance structures correspond exactly to the same total energy [46]. Figure 4 shows the two degenerate structures of *trans*-PA. The difference between the structures is an interchange of the carbon-carbon single and double bonds. The two different structures in Figure 4 have identical ground state geometries [39]. PA is the first conducting polymer to be characterised and has been the subject of many theoretical analyses. Due to its degenerate ground state, the charge carrier species in *trans*-PA are known as solitons. In effect, the neutral soliton carries no charge and posseses spin ½. A charged soliton on the other hand is spinless and is singly charged ($\pm e$) [38].

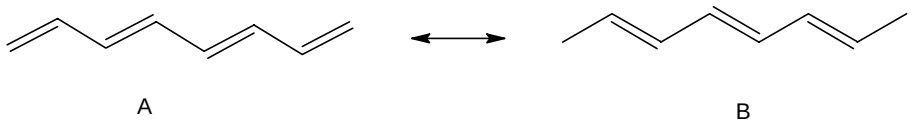

Figure 4: *Two degenerate ground state structures of trans-PA.*

The renewed interest in conducting polymers started serendipitously with the discovery of a shiny metallic-like film of PA that was formed as a result of excess use of catalyst during its synthesis [47]. Later on it was discovered that PA films could become highly conductive when exposed to iodine vapour [48]. The Nobel Prize in Chemistry for 2000 was awarded to Alan J. Heeger, Alan G. MacDiarmid and Hideki Shirakawa for the discovery and development of conductive polymers based on their discovery of how PA could be made electrically conductive. However, the use of PA in practical applications has been limited. This is mainly due to the fact that PA is unstable in air, in addition to

being insoluble and infusible. In the quest to obtain materials having superior properties to PA, attention was diverted to the study and discovery of heterocylic CPs such as polypyrrole and polythiophene.

An interesting class of CPs is those possessing a non degenerate ground state. Examples of such polymers include polyparaphenylene (PPP), polypyrrole (PPy), polythiophene (PT) and their derivatives. The ground state of such polymers corresponds to a single geometric structure (aromatic-like structure) with a lower total energy than that of the corresponding resonance quinoid-like structure [38]. Figure 5 shows the two resonance structures for PPy.

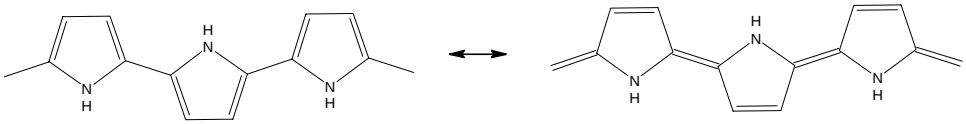

Aromatic form of PPy

Quinoid-like form of PPy

Figure 5: *Two resonance structures of PPy.*

The structures of common CPs (with non degenerate ground states) in their non-conductive form are presented in Figure 6. In their non-conductive state, the polymer backbone in these materials bears no charge. Conductivity is induced by the formation of polarons or bipolarons as opposed to what happens in the degenerate ground state systems where conductivity is due to the formation of solitons. A polaron is a radical cation or anion which has a single charge ($\pm\, e$) and ½ spin. In a higher conducting state of CPs, a bipolaron is formed, when a second electron is removed from the polymer. Formation of bipolarons is energetically more favourable than formation of two separate polarons. This is because the structural relaxation of a bipolaron is greater than that of a polaron, and redox potentials for bipolaron formation are lower than that for polaron formation [38,49]. A bipolaron is either a dication or a dianion which is spinless and doubly charged ($\pm$2 e). Combinations of techniques can be used to monitor the redox processes of CPs involving the different charge carriers including the ions responsible for charge compensation [50,51]. Of this class of non degenerate CPs, PPy was chosen to make the electroactive ion exchange membranes which were studied in this thesis. Therefore, the next sub-section is dedicated to the literature of PPy i.e. its synthesis, structure and properties.

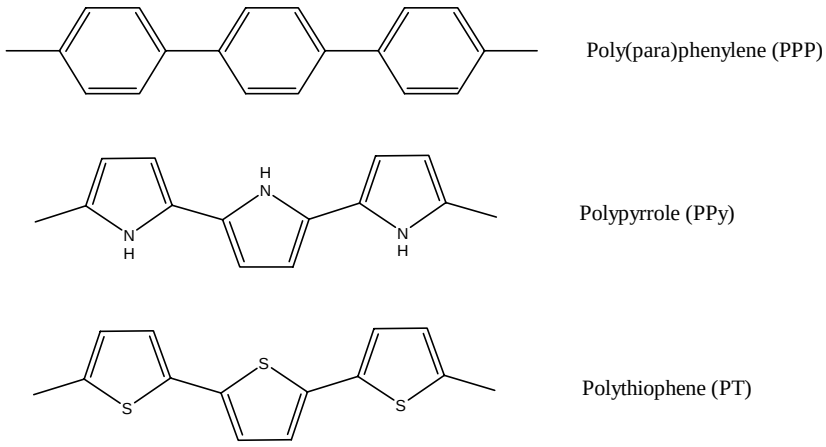

***Figure 6**: Common CPs with non degenerate ground state systems in their non-conductive/undoped state.*

3.2.2. Polypyrrole

PPy is one of the most extensively studied conducting polymers, and is synthesised by the oxidation of pyrrole (Py) or substituted Py monomers. Common routes of synthesis involve electrochemical and chemical polymerisation. The latter involves the use of chemical oxidants with the end product being in the form of a powder. The former method of synthesis involves the application of an external potential to an electrode in an electrochemical cell and results in a polymer film formed on the electrode. Electrochemical methods of preparation are clean and efficient especially for laboratory scale synthesis. Three techniques for electrochemical polymerisation are galvanostatic (constant current), potentiostatic (constant potential) and potentiodynamic (cyclic voltammetry) methods. The potentiodynamic technique involves application of a repetitive triangular potential waveform to a working electrode immersed in a solution of monomer and supporting electrolyte. This method is useful in obtaining qualitative information about the redox behaviour of the polymer during the early stages of its synthesis and also for electrochemically characterising the film after deposition. Potentiostatic growth of polymer generally results in non uniform coatings of polymer on the working electrode [13]. Galvanostatic polymerisation is carried out by application of a constant current to the working electrode. This method is advantageous in that the film thickness can be easily controlled in a simple two electrode cell system.

Consequently, this is the method of polymerisation of Py used in this thesis. The reason for this choice was the simplicity of the method (no need for a reference electrode) and the fact that the charge consumed during polymerisation can easily be followed and hence the amount of polymer deposited can be carefully controlled. Prior information about the thickness of the film is important since the rate of transport of ions is influenced by film thickness (see chapter 7).

During electrochemical synthesis, e.g. by the galvanostatic method as employed in this study, irreversible oxidation of the monomer occurs. The monomer is dissolved in an appropriate solvent containing the desired anionic doping salt. The nature of the solvent, especially its nucleophilicity, is crucial since it is known to affect the electrochemical, chemical and physical properties of the resulting polymer film [52]. Polymer films with good electrical conductivity and mechanical strength are prepared using non-nucleophilic solvents such as acetonitrile and propylene carbonate. Although water is a nucleophilic solvent, it is also a popular solvent used in electropolymerisation of pyrrole. The advantage of using water is that it can solubilise a good range of salts which provide the dopant anion needed for charge neutralisation during synthesis. In addition, water is cheap, easy to handle and safe. Electropolymerisation of pyrrole can be carried out in aqueous solution since pyrrole has a lower oxidation potential than thiophene and benzene [53,54]. Furthermore, pyrrole has a higher solubility in water than most other monomers used to prepare conducting polymers (e.g. thiophene).

The mechanism of electrochemical polymerisation of Py, as well as other heterocyclic monomers, is an $E(CE)_n$ mechanism, which begins with electron transfer (E) followed by chemical reactions (C) and electron transfer reactions (E). Concise reviews of the mechanism of electropolymerisation of Py have been written by others [49,55]. Several mechanisms have been proposed but the Diaz mechanism is perhaps the most cited in the literature. Scheme 1 shows the steps involves in the formation of a trimer according to the Diaz mechanism. The first step in this mechanism is oxidation of the monomer at the surface of the electrode to form a radical cation. The radical cation has three resonance structures, with the most stable having the highest spin density at the α-position. The next step is dimerisation or radical-radical coupling at the α-positions to form a dihydromer dication. A neutral aromatic dimer is formed by the loss of 2 H^+ from the dihydromer dication with the driving force for this step being the return to

aromaticity. Since the oxidation potential of the dimer is lower than that of the monomer, polymerisation proceeds via oxidation of the dimer. Chain propagation proceeds via electrochemical oxidation, coupling and deprotonation, until a chain termination reaction occurs.

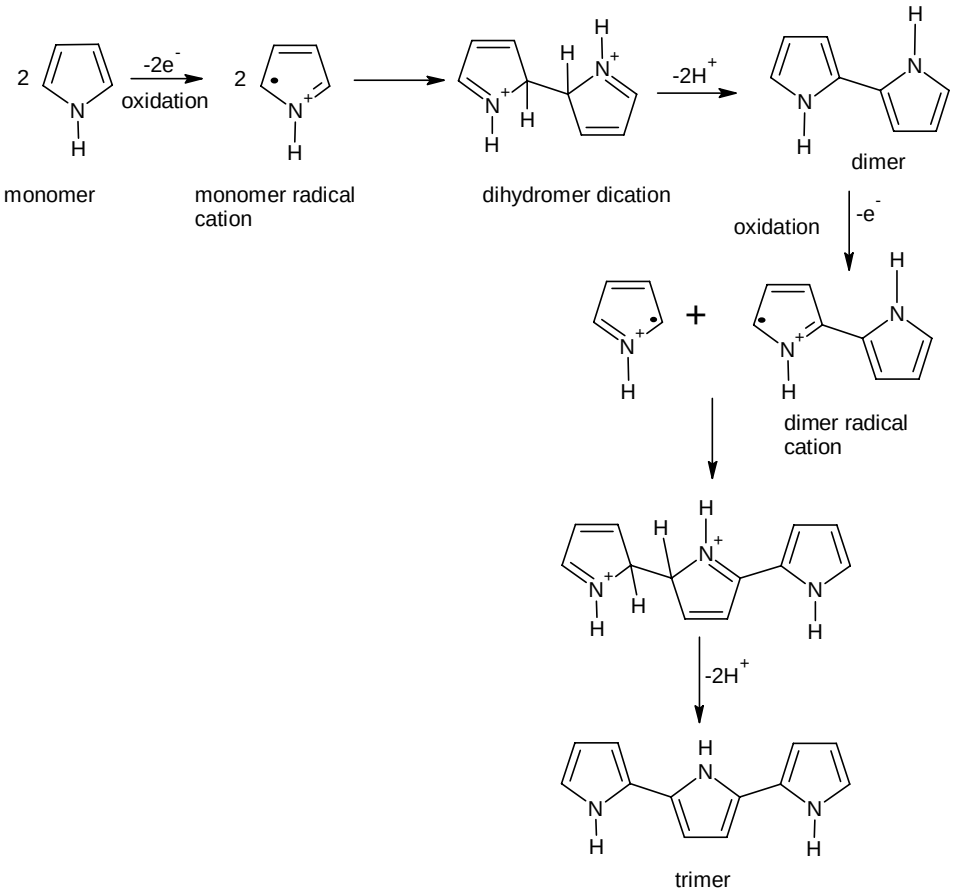

Scheme 1: Mechanism of electropolymerisation of pyrrole. From the trimer, propagation continues through oxidation, radical coupling, and deprotonation until the final polymer (PPy) is obtained.

Chain growth reactions occur in solution until eventually the chain length is such that an insoluble polymer is formed and subsequently deposits on the electrode surface [56]. The final polymer is obtained in its doped formed after oxidative galvanostatic polymerisation. The electro-oxidation reactions involve the transfer of 2 e^- per monomer unit as well as the elimination of 2 H^+ from each monomer unit, followed by the linking of the monomers at the 2,5-carbon positions. Although 2,5-linking is theoretically more favourable, the less desirable linking at the 2,3-carbon positions is also probable as

already mentioned. The polymer carries a positive charge, which is counter balanced by dopant anions. Depending on the extent of doping, every third to fourth monomeric unit of the polymer carries a positive charge [57]. This equates to the transfer of 0.25-0.33 e^- per monomer unit or a degree of doping of 25-33 %. The positive charge is delocalised over several monomer units, and the process of polymerisation and doping occurs simultaneously. Incorporation of the dopant anion during synthesis preserves charge neutrality of the polymer. An equation for the synthesis of PPy, including the loss of protons and electrons is summarised below (R6).

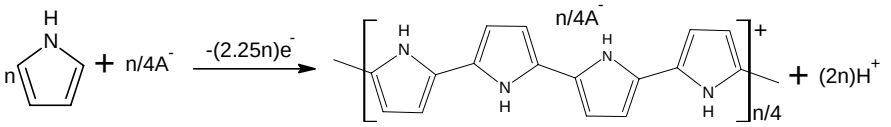

R6

Polymerisation reactions favour α-coupling, however, β-coupling is also probable in polymers with longer chain lengths. The number of β-coupling events increases with the chain length of the polymer, and also affects the degree of order of the polymer chains and therefore the degree of crystallinity of PPy [58]. Improved crystallinity has been observed with poly(3,4-dimethylpyrrole), since coupling at the β-positions is blocked by methylation.

The structure of an ideal PPy is assumed to be linear with the Py units alternately facing each other and the dopant anion incorporated between the planes of the polymer chains. This is far from the real structure which is likely to be a branched/cross linked polymer. The fact that PPy is insoluble suggests that the polymer has some degree of cross linking, and the presence of α-α linkages and α-β linkages has been observed in ^{15}N-NMR studies [59]. Soluble PPy has been obtained either by using alkyl substituted Py monomers during synthesis or by the use of specific dopant anions [60]. The substitution on Py prevents the formation of α-β linkages between monomer units. The surface morphology of PPy, as revealed by SEM studies, is typically described as cauliflower-like (nodular structure several microns in size). The surface morphology of PPy films is influenced by a number of factors including the film thickness, the nature of the solvent used during synthesis, the type of dopant anion present and the electrochemical conditions employed during synthesis. The effect on the surface

morphology of PPy of changing the dopant anion can be profound, as will be discussed subsequently in this thesis (chapter 7).

3.2.3. Doping Process

The doping process introduces charge carriers into the electronic structure of CPs, and therefore induces conductivity into the polymer. The doping process in conducting polymers is different from that of semiconductors, as it involves redox reactions [61]. Conductivity equivalent to that of metals has been realised in heavily doped CP materials [62]. Polymers can either exhibit n-type (polymer reduction) or p-type (polymer oxidation) doping or both. Examples of CPs that can undergo both n- and p-type doping are PA and PPP. PPy is a type of CP that undergoes only p-type doping. During the doping process of PPy the polymer backbone is converted to a polymeric cation by oxidative reactions that occur either chemically, electrochemically or photochemically. In electrochemical doping, the doping level can easily be controlled [62]. The electrodes provide the source and the sink for the electrons, while the electrolyte provides the doping ions needed for charge compensation. To compensate the positive charge formed on the polymer backbone during synthesis, anions need to be incorporated into the PPy matrix. Subsequently when the polymer is reduced, its backbone becomes neutral and anions that have been incorporated will be expelled to the surrounding medium. The driving force for the expulsion of anions is again charge neutrality. The oxidation and reduction of the polymer accompanying the movement of anions in and out of the polymer matrix are known as doping and dedoping. Note should be taken that there is also the possibility of the movement of cations into and out of the polymer depending on the type and size of the dopant anion used during synthesis. Also the type of ions present in the electrolyte influences the movement of the ions. The dopant anion can constitute up to 30 % of the weight of the polymer and it is obtained by carefully choosing the type of electrolyte used during synthesis. The dopant anion can either be organic or inorganic but the crucial point is that the anion oxidation potential should be higher than that of the monomer. The fact that PPy can be prepared from aqueous solutions allows for the incorporation of a greater range of dopant anions, giving rise to polymers with a wide range of properties. For example, when PPy is doped with a chiral dopant anion, a chiral conducting polymer is obtained [63,64]. PPy exhibits an anion dominating ion exchange behaviour when doped with small anions.

Recently, it was shown that a cation exchange polymer was obtained in the presence of small anion (Cl^-) due to covalent linking of the anion to the C-atom of the CP backbone [65]. A mixed ion exchange polymer is obtained when doped with medium-size anions. Cation exchange is the dominating ion exchange process for PPy doped with polyanions in the presence of electrolytes containing monovalent or divalent metal ions [66, 67]. The diverse ion exchange properties exhibited by PPy films has led to the development of electrochemically controlled PPy membrane based systems for the separation of ions between two solutions. In this thesis, the versatile nature of PPy is taken advantage of by investigating the variations in ion exchange properties that arise when different dopant anions are incorporated during electrochemical synthesis.

4. Ion Transport across Conducting Polymer Membranes

4.1. Principles

The transport of ions (electroactive and inactive) and small organic molecules across commercially available membranes coated with CPs, or free standing CP membranes, has been intensively studied over the past years. When the CP membrane is repeatedly reduced and oxidised, ions are pumped across the membrane. The important point here is that the membranes have to be electrochemically stimulated to allow the transport of ions. The permeability of the membranes towards the ions depends on a number of factors, including composition, porosity of the membrane and the type of applied stimulus. The rate of transport of ions, on the other hand, depends mainly on the size and charge of the ions [13].

The principles of operation of an electrochemically switchable membrane based on a conducting polymer, e.g. PPy, for ion transport is based on the change in oxidation state of the polymer when its potential is modulated. PPy is present in an oxidised state after it has been formed by polymerisation through electrochemical oxidative methods. As already mentioned, three different types of ion exchange properties can be achieved depending on the size of the dopant anion employed during synthesis. PPy exhibits anion exchange properties when the polymer is doped with mobile anions such as Cl^-, NO_3^-, and SO_4^{2-} as shown in Reaction 7 (R7). When the PPy (doped with a small dopant anion) is reduced the conducting polymer backbone becomes electrically neutral. In order for the PPy to remain neutral the anion that was incorporated during electrochemical synthesis must be expelled. When the polymer is reoxidised, positive charges are returned to the conducting polymer backbone and anions present in the surrounding solution (either the original dopant or other anions present in the electrolyte) are incorporated.

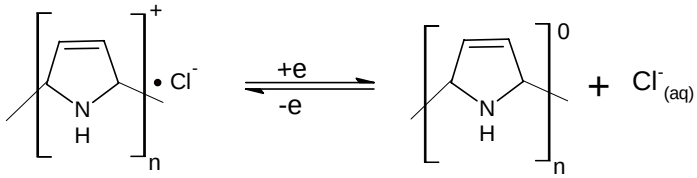

R7

In contrast, cation exchange occurs predominantly if the dopant anion is immobile or trapped within the polymer matrix. This occurs with large polyanions such as polystyrene sulphonate (PSS) and polyvinylsulphonate (PVS) and is illustrated in Reaction 8 (R8). In this case, when the polymer is reduced the conducting polymer backbone becomes electrically neutral and since the dopant anion is immobile, cations in the surrounding electrolyte are incorporated to maintain charge balance. When the polymer is subsequently reoxidised, and positive charges returned to the conducting polymer backbone, cations that were previously incorporated are expelled.

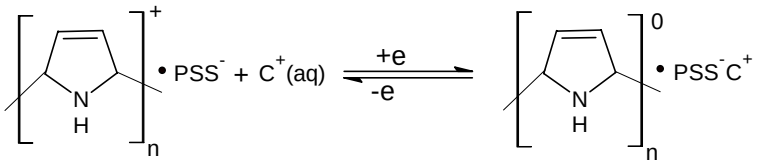

R8

A mixture of cation and anion exchange reactions is observed when PPy is doped with medium-size anions (e.g. paratoluene sulphonate (pTS)). During this process, which is illustrated in Reaction 9 (R9), both anions and cations move in and out of the polymer when the polymer is oxidised and reduced.

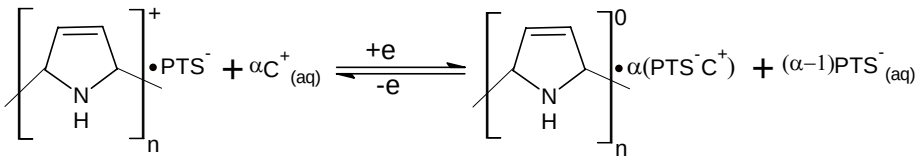

R9

The various ion exchange behaviours of CPs shown in Reactions 7- 9, can be used to develop a system by which ion transport across electroactive membranes can be achieved by electrochemical control of the membrane. In the case of an ion separation system built with PPy as the active component of the membrane, electrochemical switching enables the movement of ions from a solution on one side of the membrane to a solution on the other side. In this type of separation process, the PPy membrane is placed between the two compartments of a transport cell. The membrane acts as a barrier inhibiting the transport of ions from the source cell to the receiving cell when no potential is applied. Ion transport is only initiated when a pulsed potential is applied to the membrane. In one ideal case, a PPy membrane doped with mobile anions will be permeable only towards anions, and cations will be retained in the source solution. In a

similar way, membranes composed of PPy doped with immobile anions will be permeable only towards cations, and anions will be retained in the source solution. What is observed in practise is more complicated and far from the ideal scenario. This will be addressed later on in this thesis (chapter 7).

4.2. State of the Art: PPy as an Ion Transport Membrane

Some thirty years ago, Murray and Burgmayer were the first to demonstrate that PPy could be used as an electroactive ion exchange membrane for the separation of ions between two electrolytes. They observed that PPy membranes can permeate different ions by electrochemically switching the PPy between its oxidised and reduced states [14, 68, 69]. In their early experiments, PPy deposited on a gold minigrid porous electrode was used as an electroactive membrane for separating ions between two solutions. They called their device an 'Ion gate membrane', since the resistance of the membrane can be electrochemically controlled by altering the oxidation state of the PPy. The membrane was 'switched on' when oxidised and 'switched off' when reduced [14]. In a transport experiment in which the PPy membrane separated two compartments containing 1 M KNO_3 and 1 M KCl, direct potentiometric measurement of Cl^- proved that an anion exchange membrane was realised when PPy was in the oxidised state [69]. The permeability of reduced PPy towards Cl^- was about 50 times lower than when it was in the oxidised state. In addition, reoxidising the PPy film decreased its permeability towards Cl^- ions. This was explained to be due to the irreversible loss of cationic sites through attack by oxygen. In the same study, these researchers postulated that transport of co-ions (cations) across the membrane could occur i.e. the membranes did not exhibit complete permselectivity [69].

Cation exchange membranes based on PPy were first developed by Shimidzu et al. [11, 70 - 71]. These researchers fabricated charge controllable composite membranes containing PPy doped with polyanions and demonstrated that PPy doped with polyvinylsulphate (PVS) in contact with a solution of KCl incorporated K^+ when the polymer was reduced. It was suggested that such membranes could be used as ion selective permeable membranes whose charge can be controlled electrochemically. In addition, an electrochemical deionisation system using anion exchange (PPy(Cl)) and cation exchange (PPy(PVS)) electrodes was constructed, and its applicability

demonstrated by immersing in 10^{-3} to 10^{-4} M solutions of KCl [11]. Electrochemical deionisation and regeneration was accomplished by applying 0.03 – 1.0 mA and 0.3 mA, respectively. The concentrations of K^+ and Cl^- were measured by atomic absorption spectroscopy (AAS) and ion chromatography (IC) respectively. The calculated ion exchange capacity of PPy(Cl) and PPy(PVS) were determined as 2.1 mmol/g and 1.9 mmol/g, respectively (for monovalent ions), which are comparable to that of conventional ion exchange resins. Wang et al. followed in this direction by producing a stand-alone membrane of PPy(NO_3), which they used to investigate the transfer of monovalent cations [72]. An asymmetric ion channel model explained the transfer of ions across the PPy membrane, when it was polarised by an electric field [72,73]. In the same year, another group examined the environmental stability of composite materials consisting of chemically polymerised PPy and polyaniline (PANI) deposited on commercially available membranes (Teflon and polypropylene) [26]. However, they did not study the transport of ions across the membranes. Schmidt et al. later demonstrated that methanol can permeate across a composite membrane consisting of PPy deposited on Teflon [74]. When the polymer was reduced cations were incorporated, which led to structural changes in the film that created a more porous network structure, which further increased the permeation of methanol.

Further advances in this area of research stem from works carried out by Wallace et al. [75-90]. This group intensively studied the development of CP membrane systems for metal ion separation applications. This included examining the effect of varying the hardware and system configuration, types of membranes prepared, in situ electrochemical techniques used for switching the membrane between redox states and type of ions to be transported (electro-inactive and -active) [75-85]. It was shown that the flux of metal ions and selectivity of the membranes towards ions are influenced by the nature of the electrical stimuli applied [78]. Application of a pulsed potential waveform to the membrane resulted in higher metal ion fluxes, while the pulse width also had an influence on the selectivity of the membranes towards different ions [78]. Initial studies were performed using stand-alone conducting polymer membranes for the transport of metal ions [76-86], and charged organic molecules [87]. Due to the limited strength and porosity of these stand-alone membranes, new composite membranes using PVDF as a support substrate were developed [85, 86, 88, 89]. Transport of different types of metal ions, including alkali metal ions, alkaline earth metal ions and transition

metal ions across composite membranes based on polypyrrole [85, 86, 88, 89], polyaniline [78] and poly(bithiophene) [90] were investigated.

Along the way other researchers also got involved in the development of membrane separation systems based on PPy. For example, Jüttner et al. worked on the development of an anion/cation permeable membrane based on PPy [91,92]. They stipulated that permeation of anions can be observed when PPy is in its oxidised state, while cation permeability is observed when PPy is reduced [91]. Shahi et al. built an electrodialysis system based on PPy deposited on a conventional ion exchange membrane in order to investigate the selective permeation of monovalent ions over divalent ions [93]. The permeability of nitrate ions across a PPy stand-alone membrane, when the polymer was in the oxidised state, was demonstrated by Otero et al. [94]. The ionic conductivity of free standing PPy films was measured and it was concluded that it depended on the concentration of the electrolyte and degree of oxidation of the PPy film. An electrochemically stimulated conformational relaxation (ESCR) model was used to explain that PPy in its fully oxidised state has a relaxed/swollen polymeric structure, across which ions move more easily than with a reduced PPy, which has a more compact structure [95].

To improve permeability towards transition metal ions, Ralph and co-workers developed membranes based on PPy doped with metal complexing anions [88, 89]. It was shown that transition metal ions, e.g. Co^{2+}, Ni^{2+} and Zn^{2+}, could be transported across composite membranes based on PPy doped with bathocuproinedisulphonic acid (BCS) [88]. This membrane was also found to be permeable to a number of other metal ions such as K^{+}, Mg^{2+}, Ca^{2+}, Mn^{2+}, Fe^{3+} and Cu^{2+}. Previous studies with other PPy membranes have shown that they are also permeable towards transition metal ions such as Cu^{2+} [84], Fe^{3+} and Mn^{2+} [76]. However, the flux of these metal ions across composite membranes containing PPy(BCS) was much higher. For example, the flux of Cu^{2+} ions through PPy(BCS) membranes was reported to be about 50 times higher than with previously studied PPy membranes [88]. The same group also developed composite membranes based on PPy doped with sulphated cyclodextrins (CDS) [89]. The results obtained from transport experiments performed with these new membranes demonstrated that composite membranes containing PPy(CDS) are about 10 times more permeable towards Mn^{2+}, Co^{2+}, Ni^{2+} and Zn^{2+} than membranes composed of PPy doped

with 8-hydroxyquinoline-5-sulphonic acid (HQS) or BCS. Similar permeabilities had not been observed with any other previously studied conducting polymer membrane. Milestones in the research of PPy as ion transport membranes from its birth in 1982 to the current date are shown in Figure 8.

After a brief recess in research in this area, the group of Ivaska in collaboration with the University of Wollongong continued work towards the development of PPy membranes in order to improve their permeability and/or selectivity towards divalent and transition metal ions (Paper II, IV). In the course of this work, some key issues vital for the development of membrane systems based on CPs was addressed (Paper I, III, and V). The main issues discussed in Papers I – V has been combined to form the framework of this thesis.

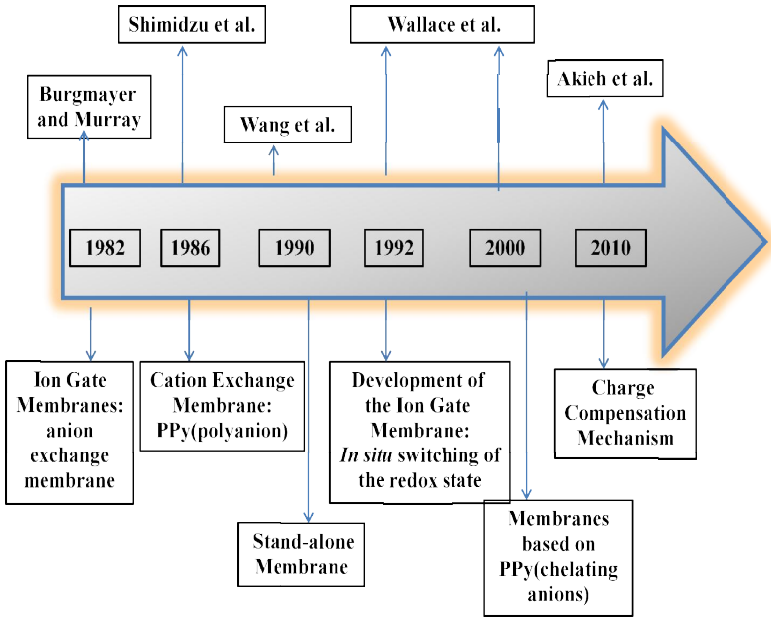

Figure 7: *Milestones in the study of ion transport across PPy membranes.*

5. Aim and Hypothesis of the Study

The main focus of this thesis was to develop electroactive cation transport membranes containing polypyrrole for the separation of metal ions between two solutions in a two compartment transport cell. Membranes under study consisted of composite membranes containing PPy films deposited on commercially available support materials. The specific aims of the study were:

1) To prepare and characterise electroactive cation transport PPy membranes.
2) To investigate the permeability of PPy membranes towards divalent and/or transition metal ions.
3) To investigate the mechanism of ion transport across PPy membranes.
4) To investigate the mechanism of macroscopic charge compensation in the receiving solution during the transport of ions across PPy membranes.

In order to carry out these tasks, cation exchange membranes consisting of PPy doped with immobile anions were prepared. Chemical structures of the dopant anions used in preparing composite membranes containing PPy used in this thesis are shown in Figure 8. Four types of dopant anions were used, however only two of these, namely 4-sulfonic calix[6]arene (C6S) and carboxylated multi-walled carbon nanotubes (CNT), were presumed to exhibit a degree of selectivity for divalent metal ions. 4-sulphonic calix[6]arene (Figure 8a) was expected to be a suitable dopant for preparing cation exchange membranes containing PPy because of its bulky size, solubility in water and overall negative charge. In addition, due to the flexible internal cavity of the calixarene, it could be expected to complex a variety of metal ions, provided that the complexing property of the ligand is preserved after entrapment in the polymer matrix. Similar expectations were derived after considering the properties of carboxylated multi-walled carbon nanotubes (Figure 8b). These negatively charged CNTs suspension can act as both the background electrolyte and the dopant anion during electrochemical polymerisation of Py. It was expected that the presence of carboxyl groups in the resulting membranes might increase the strength of their interactions with divalent metal ions. The PPy(CNT) membranes were expected to show greater permeability towards metal ions since it is known that composite films composed of PPy(CNT) exhibit superior electrochemical properties, including higher conductivities and

capacitances, compared to PPy films doped with non-conductive anions e.g. polystyrene sulphonate (Figure 8c) and para-toluene sulphonate (Figure 8d).

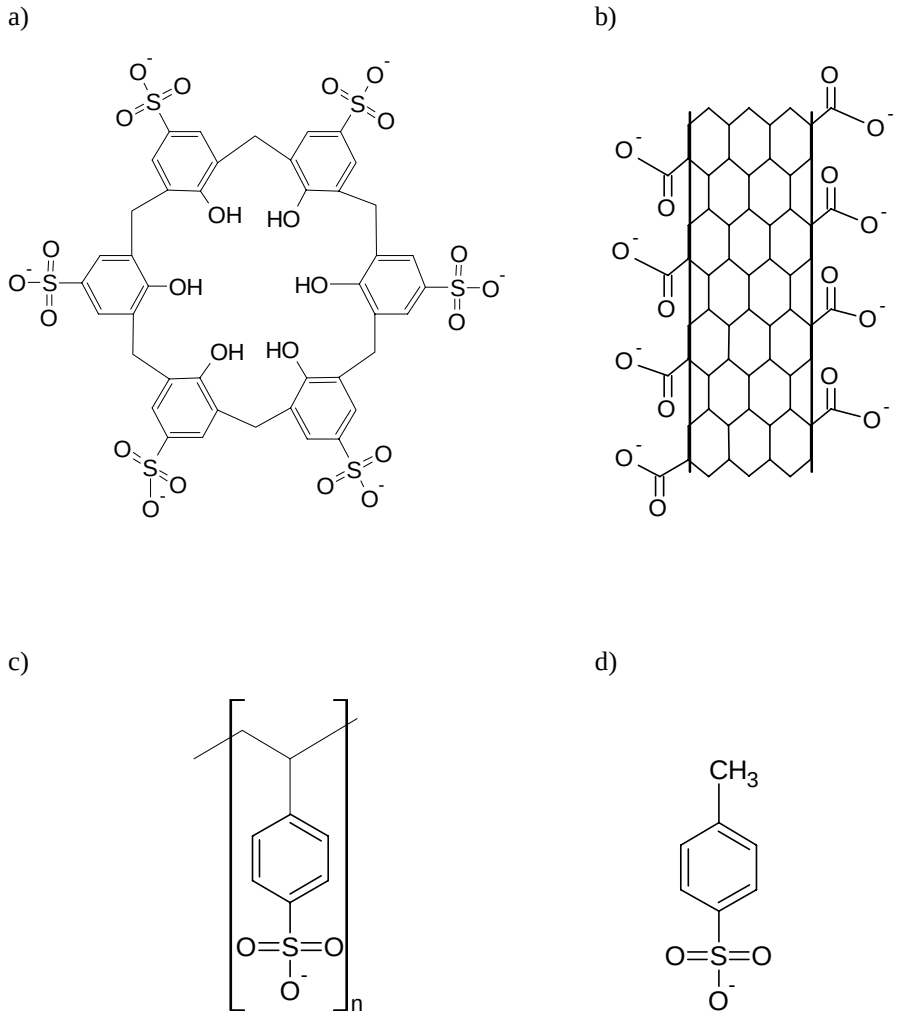

Figure 8: *Chemical structures of dopant anions used in preparing composite PPy membranes: (a) 4-sulphonic calix[6]arene, (b) carboxylated multi-walled carbon nanotubes, (c) polystyrene sulphonate and (d) para-toluene sulphonate.*

The reason for studying the macroscopic charge balance was to understand the extent of permselectivity in PPy membranes. It was postulated that PPy cation exchange membranes that exhibit permselectivity would be permeable only towards cations, while PPy anion exchange membranes would be permeable only towards anions. If this hypothesis were true, it would be important to understand how the excess charge arising from the permeated anions and cations is neutralised in the receiving solution (Figure 9).

In order to address this question, it was assumed that either the membranes were not permselective or there was an additional process, e.g. electrolysis of water, which would introduce additional cations and anions into the receiving solution.

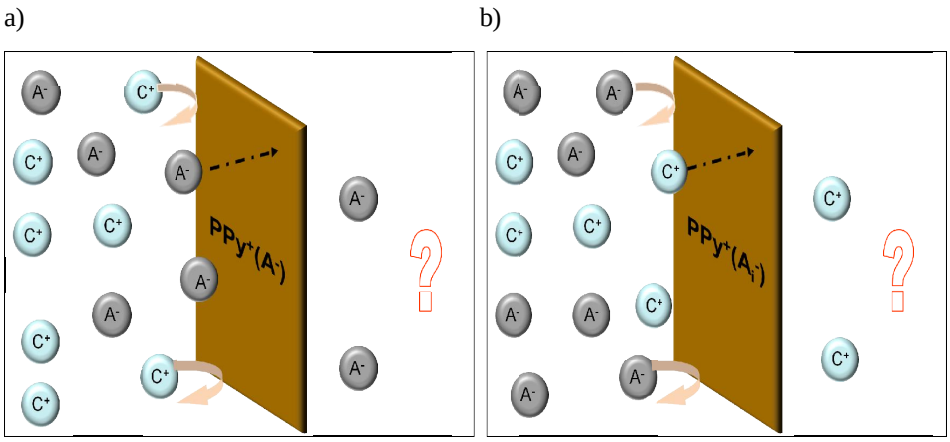

Figure 9: *Polypyrrole membrane demonstrating permselectvity (a) anion exchange membrane (b) cation exchange membrane.* A^- *is a mobile (dopant) anion,* A_i^- *is an immobile dopant anion and* C^+ *is a cation.*

6. Experimental Section

6.1. Membrane Preparation

A thin film of platinum was sputter-coated on polyvinylidene difluoride (PVDF) and Nucleopore® track-etched polycarbonate (PC) membranes using a BAL-TEC SCD 050 sputter coater. The operating conditions for sputtering platinum on PVDF were either 40 mA for 450 s, or 30 mA for 900 s. For PC, sputtering was performed by applying a current of 40 mA for 300 s. Sputtering was performed to render the PVDF and PC support membranes electrically conductive. The average pore size diameter and thickness of the PVDF was 0.22 µm and 100 µm, respectively. The PC membranes, on the other hand, had a more uniform pore size of 0.1 µm and were much thinner than the PVDF membranes (6 µm thick). PPy films were prepared on each support material. Electropolymerisation was performed in all instances galvanostatically at 23±1°C using an AutoLab PGSTAT 20 potentiostat/galvanostat. The current density and polymerisation time determined the thickness of the final polymer film. The composition of the polymerisation solution depended on the type of dopant anions to be used. Table 1 shows the composition of the polymerisation solution and the current densities used for preparing different polymer films. For transport studies, 5 different types of PPy films were prepared. These were PPy doped with 4-sulphonic calix[6]arene (PPy(C6S), PPy doped with carboxylated multi-walled carbon nanotubes (PPy(CNT)), PPy doped with polystyrenesulphonate (PPy(PSS)), PPy doped with para toluene-4-sulphonate (PPy(pTS) and PPy doped with perchlorate (PPy(ClO_4)).

***Table 1**: Composition of electropolymerisation solutions and polymerisation conditions.*

Target Polymer	Py concentration (M)	Electrolyte concentration	Current density (mA/cm^2)	Time (mins)
PPy(C6S)	0.2	1.7 mM C6S	1	10-30
PPy (CNT)	0.6	0.1% (w/v) CNT	0.05-0.1	60, 120
PPy (PSS)	0.2	0.1 M NaPSS	1	60
PPy(pTS)	0.2	0.05 M pTS	1	15, 30
PPy(ClO_4)	0.2	0.1 M $LiClO_4$	1	60

The polymerisation solutions generally consisted only of the monomer, Py, and the electrolyte. However, in order to prepare PPy(PSS) and PPy(CNT), 1 mM dodecylbenzene sulphonate (DBS) was added to the polymerisation solution in order to produce pin hole-free films [96]. In addition, DBS served as an additional background electrolyte for the preparation of PPy(CNT). Bilayer polypyrrole films were also prepared in which the bottom layer consisted of PPy(pTS), and the top layer PPy(CNT). PPy(pTS) was prepared from a solution containing 0.2 M Py and 0.05 M pTS, by applying a current density of 1 mA/cm^2 for 15 min. PPy(CNT) was prepared from a solution containing 0.6 M Py and 0.1% (w/v) CNT by applying a current density of 0.05 mA cm^{-2} for either 1 or 2 h. The performance of the bilayer membranes was compared to that of a single layer of PPy(pTS) prepared under identical conditions. Prior to electropolymerisation all solutions were deoxygenated with argon for 10 min. A two-electrode cell shown schematically in Figure 10 was used to perform electropolymerisations. This consisted of the platinised support membrane in contact with a platinum wire acting as the working electrode and either a piece of stainless steel mesh or a glassy carbon rod as the counter electrode. The active area of the working electrode was either 7.03 cm^2 or 15 cm^2. When the larger surface area working electrode was employed, stainless steel mesh was used as the counter electrode. After polymerisation, the membranes were washed thoroughly with deionised water in order to remove any remaining monomers, oligomers, electrolyte and other impurities.

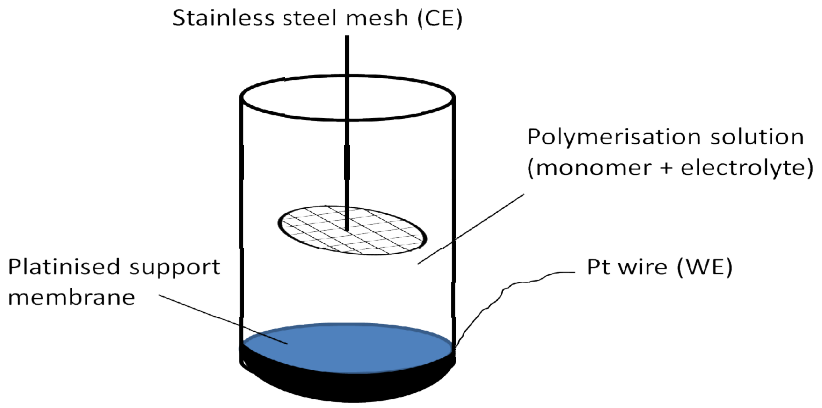

Figure 10: *Schematic illustration of the electropolymerisation cell used to prepared polymers. CE = counter electrode and WE = working electrode.*

6.2. Membrane Characterisation

6.2.1. Electrochemical Quartz Crystal Microbalance

Electrochemical quartz crystal microbalance (EQCM) is a technique which combines QCM with electrochemical stimulation of a material [97-100]. It is a sensitive technique in which small changes in mass of an electroactive material can be detected by measuring variations in the oscillation frequency of a quartz crystal on which the material is deposited [101]. The technique is based on the converse piezoelectric effect of a quartz crystal, whereby the application of a voltage across the crystal causes a corresponding mechanical strain [102]. An alternating electric field applied between two metal electrodes deposited on each face of the crystal causes it to oscillate in parallel to its surfaces. The resonant frequency of this oscillation is inversely proportional to the mass change of the crystal. The relationship between the change in mass per unit area (Δm) and the change in frequency (Δf) is given by the Sauerbrey equation (Equation 1, Eq 1).

$$\Delta f = \frac{-2\Delta m n {f_0}^2}{A\sqrt{\mu_q}\rho_q} \qquad \text{Eq 1}$$

In this equation, f_0 is the resonant frequency of the crystal, n is the overtone number, A is the area of the working electrode, μ_q is the shear modulus of the crystal and ρ_q is the density of the crystal. Eq 1 can be rewritten as Equation 2 (Eq 2).

$$\Delta f = -C_f \Delta m \qquad \text{Eq 2}$$

In this equation, C_f is a constant related to the sensitivity factor of the crystal. According to this relationship, if the mass of a crystal increases the resonant frequency will decrease.

The Sauerbrey equation assumes that the film is thin and uniformly deposited on the crystal. Also, the crystal and the film (e.g. PPy film) should behave as a rigid entity, since changes in frequency can also be caused by viscoelastic effects of the film [103]. Quantitative interpretation of EQCM data is achieved through consideration of the Sauerbrey equation in combination with Faraday's law [101]. Faraday's law relates the charge passed during the electrochemical reaction (Q) to the number of moles of

material electrolysed (N) [104]. This relationship is used to obtain information about what species are involved in the mass changes occurring during redox reactions of PPy films. Faraday's law can be written as shown in Equation 3 (Eq 3).

$$Q = nFN \qquad \text{Eq 3}$$

In this equation, n is the number of electrons involved in the electrochemical reaction and F is the Faraday constant. Combining Eq 2 and Eq 3 gives Equation 4 (Eq 4) which relates the change in frequency to the charge passed during an electrochemical reaction.

$$\Delta f = \frac{-M' C_f Q}{nF} \qquad \text{Eq 4}$$

Equation 4 can be rewritten as Equation 5.

$$\Delta m = \frac{M'}{zF} Q \qquad \text{Eq 5}$$

In this equation, M' is the apparent molar mass of the species causing the change in mass on the PPy film, z is the charge on the transferred ion and Q is the charge consumed during the reaction. The slope of a plot of Δm against Q can be used to compute the apparent molar mass of the ions involved in charge compensation during oxidation and reduction of the PPy films. Only the linear region of the plot of Δm against Q is taken into consideration when calculating the apparent molar mass.

The EQCM experiments carried out in this thesis were performed with either 9 MHz AT-cut, polished, quartz crystals coated with Ti and Pt (INFICON, Inc., USA) or 5 MHz AT-cut, polished, quartz crystals coated with Cr and Au electrodes (Coherent Scientific, South Australia). The crystals had an overall diameter of 2.54 cm and an electrochemically active surface area of 1.37 cm^2. The set-up used for performing EQCM experiments is shown in Figure 11.

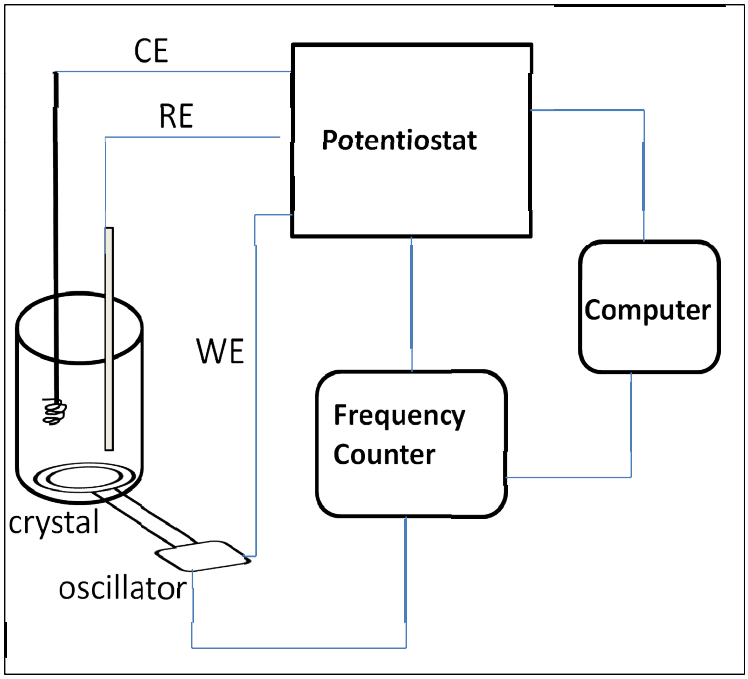

Figure 11: *Set-up for performing EQCM experiments. CE = counter electrode, RE = reference electrode, WE = working electrode.*

9 MHz AT-cut, quartz crystals were used in conjunction with a Maxtek plating monitor to investigate the ion exchange properties of PPy(CNT) and PPy(C6S) films immersed in 0.1 M KNO_3, 0.1 M $Ca(NO_3)_2$ and 0.1 M $Mn(NO_3)_2$ solutions. Films were cycled between -0.85 V and +0.6 V at scan rates of 100 mV/s, 50 mV/s and 10 mV/s. Experimental conditions used during polymerisation of PPy on the surface of the quartz crystals and subsequent characterisation, are reported in the experimental sections of Paper IV for PPy(CNT) and Paper V for PPy(C6S). The composition of the polymerisation solutions and electrochemical conditions used for preparing each film are shown in Table 2. Film thickness was controlled during polymerisation by following the increase in mass of the crystal. Polymerisation was stopped manually when the mass of the crystal reached a certain value that indicated the target thickness of the film has been reached (Table 2). The sensitivity factor for the crystal employed in these experiments was 0.13 Hz ng^{-1}. The thickness of the PPy films was kept below 1 µm to avoid deviations from the Sauerbrey equation [105,106].

Table 2: *Composition of polymerisation solutions and electrochemical conditions used for growing PPy films for EQCM studies.*

Polymer	Py concentration (M)	Electrolyte concentration	Current density (mA/cm^2)	Time (s)	Mass (µg)	*Thickness (nm)
PPy(CNT)	0.6	0.1% (w/v) CNT	0.2	300	34.3	340
PPy(C6S)	0.2	1.7 mM C6S	0.5	72	27.4	270
PPy(pTS)	0.2	0.05 M pTS	0.5	300	-	450¤
PPy(PSS)	0.2	0.1 M PSS	0.5	300	-	450¤

**The density of the film was assumed to be 1 g/cm^3.*
¤The film thickness was calculated from the amount of charge passed during polymerisation (205.5 mC).

The ion exchange behaviour of PPy(PSS) films and PPy(pTS) films was investigated using a 5 MHz AT-cut, polished, quartz crystal, with chromium/gold electrodes obtained from Coherent Scientific, South Australia. Polymerisation solutions and electrochemical conditions used in preparing PPy(pTS) films and PPy(PSS) films are shown in Table 2. Charge compensation experiments with PPy(PSS) were performed in 0.1 M aqueous solutions of KNO_3, $Ca(NO_3)_2$, $Co(NO_3)_2$, $Mn(NO_3)_2$, $Cr(NO_3)_3$, and $Al(NO_3)_3$. This set of solutions was chosen as it encompassed mono-, di- and trivalent metal ions. A PAR363 poteniostat/galvanostat was used to apply a triangular potential waveform to the working electrode, with the potential cycled between −1.0 V and +0.7 V, and the scan rate 100 mVs^{-1}, for 100 cycles. The experimental conditions used during polymerisation and characterisation for PPy(PSS) films are reported in Paper I.

6.2.2. Scanning Electron Microscopy and Energy Dispersive X-ray Analysis

Scanning electron microscopy (SEM) in combination with energy dispersive X-ray analysis (EDXA) is a powerful set of tools that provides morphological and topographical information about the surfaces of materials, while simultaneously also giving qualitative and quantitative information about the elemental composition.

In SEM an incident beam of electrons is scanned over the surface of a sample. The electrons interact with the atoms on the surface and generate signals which are collected to produce information about its morphology and composition. The source of the electrons can be a heated tungsten filament, lanthanum hexaboride (LaB_6) filament or a field emission gun. A Schottky field emission gun was the source of electrons in the instrument used in this thesis. When the incident electrons strike the surface of the

sample, a number of different types of effects occur including production of backscattered electrons, secondary electrons and X-rays. Each of these can be detected by special detectors [107]. The backscattered and secondary electrons are used to generate microscopic images, while the X-ray photons are used to identify the elements present. Incident electrons which interact with the sample surface and exit without any loss in energy (i.e. elastic scattering) are referred to as backscattered electrons. The beam of backscattered electron has a larger diameter than that of the incident beam, and produces images with a high degree of atomic number contrast. Along with backscattered electrons, secondary electrons are also generated. Secondary electrons have lower energy compared to the incident electrons (from several keV to about 50 eV or less) [107,108]. High resolution microscopic images can be obtained with secondary electrons but these electrons are emitted only from a depth of 50 to 500 Å below the surface of the sample, thus restricting information obtained to this region of the sample. When the incident electron knocks out an electron from an inner shell of an atom, an electron from the outer shell will fall back to replace the lost electron. The energy that is released in this process is emitted in the form of an X-ray photon, which can be detected by an energy dispersive X-ray detector. The wavelength of the emitted X-ray radiation is characteristic for each element.

A Leo Gemini 1530 scanning electron microscope having a ThermoNORAN x-ray detector was used in this thesis to obtain the images shown and thereby provide information about the morphology and thickness of PPy films (Papers II-IV). Cross sections of freshly prepared composite membranes were used to determine the membrane thickness. The morphology of the surface of the membranes was investigated before and after they were used in transport studies. Elemental analyses of the membranes were obtained simultaneously (Papers II-V).

6.3. Transport Studies

Prior to transport experiments, composite PPy membranes containing a hydrophobic support material (PVDF) were soaked in 1:1 ethanol:water to improve their wettability, and then carefully assembled in the transport cell. In contrast, composite PPy membranes containing PC did not require this treatment. A freshly prepared membrane was used for each transport experiment, which was performed using the cell shown schematically in Figure 12. The transport cell consisted of two compartments separated by the composite membrane. Two types of transport cells were used which differ in volume of the cells (15 ml or 75 ml). The active area of the membrane for the bigger cell was 8.05 cm^2, while that for the smaller cell was 1.77 cm^2. The bigger cell was used for the experiments described in Papers II and III, while the smaller cell was used for the work presented in Paper IV.

The source cell contained 0.1 M metal nitrate solution, while deionised water was present in the receiving cell. A Ag/AgCl (3 M NaCl) reference electrode and either a gold coil wire or a reticulated vitreous carbon (RVC) counter electrode were placed in each cell. The composite membrane served as a common working electrode for both cells. In order to investigate if metal ion flux across the membrane can be electrochemically controlled or not, the transport experiments were performed in three stages. During Stage 1, no electrical potential was applied to the membrane, while in Stage 2 a pulsed potential waveform was applied (-0.8 V to + 0.5 V, 50 seconds pulse width). Finally, during Stage 3 no potential was again applied to the membrane. The change in concentration of metal ions or anions in the receiving solution was monitored either continuously with an ISE inserted in the receiving solution or by withdrawing aliquots for analysis every 30 minutes. In order to maintain constant volume in this compartment, the volume of solution that was withdrawn from the receiving cell was replaced with the same volume of deionised water. The concentration of metal ions was determined by inductively coupled plasma-optical emission spectroscopy (ICP-OES), while the concentration of anions was determined by ion chromatography (IC).

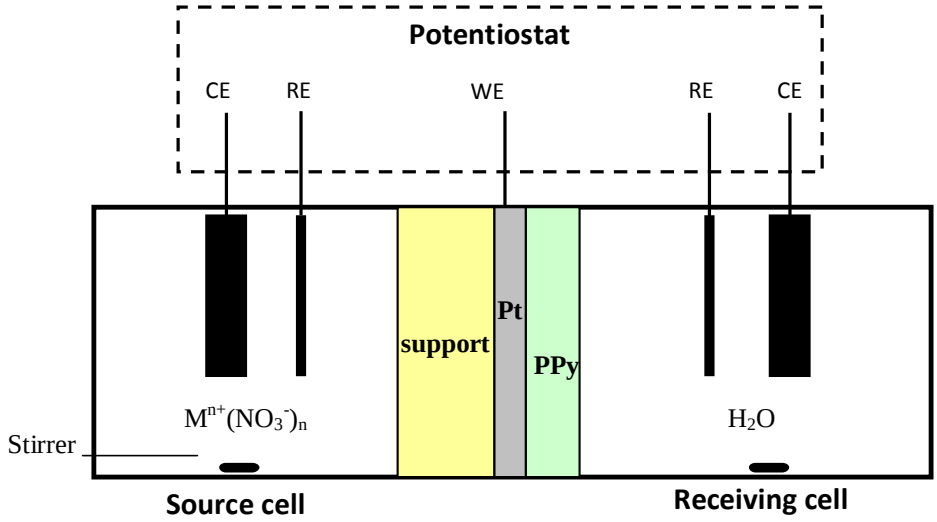

Figure 12: *Schematic illustration of the transport cell used to examine the permeation of ions across PPy composite membranes. CE = counter electrode, RE = reference electrode, WE = working electrode, M^{n+} represents the metal ions under study.*

6.4. Analysis of Metal Ions and Anions

6.4.1. Inductively Coupled Plasma-Optical Emission Spectroscopy

In inductively coupled plasma-optical emission spectroscopy (ICP-OES), the source for atomisation and ionisation is plasma, which is a highly energetic ionised gas that is typically argon. The sample to be analysed is introduced into the plasma, where it is atomised and ionised. The resulting excited state atoms and ions decay to lower energy levels by emitting photons at specific wavelengths. The intensity of light emitted at these specific wavelengths is measured and is used to determine the concentration of elements present in the sample. An advantage of this method over atomic absorption spectroscopy is the use of very high temperature plasma, which can excite several different elements in the sample at the same time. This makes it possible to simultaneously measure the emission of several different elements and therefore determine their concentrations at the same time. Another advantage of this method is that it is possible to choose from several different emission wavelengths for a given element to suit the particular sample being analysed. A disadvantage of this technique is the increase in interference that can sometimes be caused by the difficulty in separating emission lines from many elements which are very close in wavelength [109].

The ICP-OES instrument used in the analyses described in this thesis was a Perkin Elmer Optima 5300 DV. The following instrumental parameters were set as default values for concentration measurements: nebulizer flow 0.8 L/min, auxiliary gas flow 0.2 L/min, plasma gas flow 15 L/min and plasma power 1300 W. Liquid samples were introduced into the nebuliser, which converts the liquid into an aerosol. The aerosol is then transported into the plasma, where it is desolvated, vaporised, atomised and excited and/or ionised [109]. Axial/end-on viewing of the plasma was employed for all the metals studied in this work except potassium, which was examined using radial/side-on viewing of the plasma. The light emitted by the excited state atoms and ions was collected and separated into different wavelengths. The concentrations of K, Mn, Co and Cr were determined at their respective emission wavelengths of 766.490 nm, 257.610 nm, 228.616 nm and 267.714 nm. However, for Ca, two emission wavelengths were used depending on the concentration range of the metal samples being analysed. These were 393.364 nm for solutions with [Ca] ≤ 1 ppm and 317.933 for solutions with [Ca] > 1 ppm. A multi element standard was used as the calibration solution, and the samples to be analysed were diluted by a factor of 5 prior to ICP-OES measurements.

6.4.2. Ion Chromatography

Ion chromatography (IC) is a combination of two well-established techniques, i.e. ion exchange chromatography and conductivity measurements [110]. An ion exchange column is employed to separate different ions present in the solution, while the conductivity meter detects and quantifies the ions after their separation.

In this thesis, IC was employed to determine the change in concentration of anions present in the receiving solution through the course of transport experiments. The instrument used was a 761 compact IC 1.1 instrument (Metrohm AG Switzerland) connected to a conductivity detector. In order to perform an analysis, 20 µL of sample was injected into the separator column (Metrosep anion Dual 2), where the anions present interact with the ion exchange sites of the ion exchange resin. The ion exchange resin is an anion exchange material made from polymethacrylate with quaternary ammonium groups. The eluent consisted of a mixture of 2 mM $NaHCO_3$ and 1 mM Na_2CO_3 and was pumped through the column at a flow rate of 0.8 mL/min. Elution of

anions occurred at different retention times depending on the strength of binding to the column as reflected in the magnitude of the ion exchange equilibrium constant. After leaving the anion exchange column, the eluted solution travels to the suppressor column, which contains a cation exchange resin that captures the metal ions and replaces them with H^+. A unique aspect of this instrument is the state-of-the-art tri-chamber suppressor technology which provides a fresh suppressor chamber for each measurement. Complete regeneration of the chamber after each sample ensures highly efficient cation exchange reactions. A 0.1 M H_2SO_4 solution and deionised water was used for regeneration and washing the suppressor column, respectively, after each sample. The role of the suppressor column is to reduce the conductivity of the background electrolyte and eliminate counter ions. This is important in enhancing the sensitivity of detection towards anions and increasing the signal to noise ratio in the chromatograms obtained. The suppressor column converts the highly conducting eluent ($NaHCO_3$ and Na_2CO_3 solutions) into undissociated carbonic acid solution. Quantification of the anions present in the suppressed electrolyte is then achieved using the conductivity detector. A calibration curve is obtained using the peak areas generated by the conductivity detector for a series of standard solutions of known concentration.

6.4.3. Ion Selective Electrode

An ion selective electrode (ISE) is a type of electrochemical sensor, in which the potential difference between the ISE and a reference electrode (constant potential) is measured under zero current conditions [111, 112]. In a typical set-up for measuring ion concentrations, the ISE and the reference electrode are connected to a sensitive milli-volt potentiometer with a high input impedance to minimise electrical flow through the circuit. Ion/molecular recognition is performed by the ion selective membrane (ISM), hence the name ion selective electrode. In a conventional ISE the membrane separates the sample solution from the internal filling solution. The target ions from the sample solution diffuse into/out of the membrane and a potential difference arises at the membrane/solution interface, owing to charge separation due to selective binding and different ion mobilities of the ionic species.

The Nernst equation (Equation 6, Eq 6) shows that the potential of the sensor is directly proportional to the logarithm of the activity of the target ions in the sample solution.

$$E = E^0 + 2.303\frac{RT}{z_i F}\log a_i(aq) \qquad \text{Eq 6}$$

In this equation, R is the universal gas constant, T is the absolute temperature, F is the Faraday constant, E^0 is the standard potential, a_i is the activity of the target ion and z_i is the charge of the target ion. The quantity $2.303\frac{RT}{z_i F}$ is obtained from a slope of a plot of E vs log a_i and reflects the sensitivity of the electrode in milli-volts per decade of concentration and is used to verify that the ISE is functioning correctly, i.e., if it is a Nernstian response. For monovalent cations (z_i=1) and divalent cations (z_i=2) the slope is expected to be 59 and 29 mV per decade, respectively at 25^{o}C for a Nernstian response.

Conventional ISEs are based on polyvinyl chloride (PVC) membranes containing an ionophore, a hydrophobic anion and other additives along with an internal filling solution and built-in reference electrode. Attempts to eliminate the internal reference electrodes and internal filling solutions from ISEs led to the invention of all solid-state ISEs. In this thesis, an all solid-state Ca^{2+} selective electrode was used to follow the change in Ca^{2+} concentration in the receiving solution during transport experiments. The source solution for these experiments contained 0.1 M $Ca(NO_3)_2$, while the receiving solution was 1 ppm Ca^{2+} solution. Prior to performing the transport experiments reported in Papers II, III and IV, preliminary experiments were performed to determine the minimum thickness of PPy required to make the composite membranes impermeable to ions under open circuit potentials. In order to do this several different PPy films were prepared using different current densities and polymerisation times. In Paper II, the effect on metal ion flux of applying a constant potential to a PPy(C6S) membrane was investigated using source solutions containing calcium nitrate. Negative and positive constant potentials were applied to the membrane and the resulting change in Ca^{2+} concentration in the receiving solution was monitored using a Ca^{2+}-ISE over the course of 1 hour.

7. Results and Discussion

The effect of preparing PPy membranes containing different dopant anion on the permeability of the membranes towards different metal ions was studied. The dopant anions studied were pTS, PSS, C6S and CNT. The focus of this study was on relatively large and bulky anions because they were expected to be relatively immobile and therefore instil cation exchange capabilities into the PPy films. In order to gain a thorough understanding of how the metal ions permeate across the various membranes, an EQCM investigation designed to shed light on the ion exchange properties of the PPy films was carried out. In addition, elemental analysis of the films was obtained to demonstrate the mobility of the dopant anions after potential cycling in a solution containing the metal ions of interest. SEM was used to study the surface morphology and determine the thickness of the PPy films. PPy(CNT) membranes were used as a model system to investigate the effect of varying various parameters on the transport of metal ions. Finally, the mechanism of macroscopic charge balance in the receiving solution was studied using PPy films known to exhibit predominantly cation exchange (PPy(PSS)), predominantly anion exchange (PPy(ClO_4)) and a mixture of cation and anion exchange properties (PPy(pTS)).

7.1. Influence of Dopant Anions on Film Properties

7.1.1. Ion Exchange Property

The ion exchange behaviour of PPy(PSS), PPy(C6S), PPy(pTS), PPy(CNT) films was studied by EQCM in nitrate solutions containing mono and divalent cations. The cations involved were alkali metal ions, alkaline earth metal ions and transition metal ions. Papers I, IV and V present EQCM studies for PPy(PSS), PPy(C6S), and PPy(CNT) films, respectively. Paper I also includes the results of studies into the ion exchange behaviour and mechanism of charge compensation for PPy(PSS) films immersed in electrolytes containing trivalent cations, namely, $Cr(NO_3)_3$ and $Al(NO_3)_3$. Papers I and V show how the ion exchange behaviour of the films changes with multiple redox cycling and variation in scan rates. In this thesis, the discussions of the latter behaviours are mainly focused on studies performed in an electrolyte containing K^+. Related studies with other electrolytes containing metal ion such as Ca^{2+}, Mn^{2+}, Co^{2+}, Cr^{3+} and Al^{3+} are found in Papers I, IV and V.

Figure 13a shows the 3rd scan obtained during a cyclic voltammetry experiment and accompanying mass changes for a PPy(PSS) film immersed in 0.1 M KNO_3. There was an initial small decrease in mass when sweeping the potential from +0.7 V in negative potential direction. Further decrease in potential led to an increase in mass which is related to the movement of cations inside the PPy(PSS) film to maintain charge balance. Reversing the potential towards the positive potential led to a decrease in mass, arising from the egress of cations from the film to compensate the positive charge that had been restored to the polymer backbone after being reoxidised. Other workers have demonstrated the same behaviour is exhibited by PPy(PSS) films immersed in electrolytes containing $CaCl_2$ [113] or perchlorate salts of various alkali metal ions and alkaline earth metal ions [67]. There is also evidence of movement of nitrate ions in and out of the PPy(PSS) film in the capacitive region of Figure 13a. However, the movement of cations in and out of the polymer in the faradaic region dominates the observed data. Equation 5 was used to compute the apparent molar mass of the ions involved in charge compensation during the redox processes undergone by the PPy(PSS) film immersed in 0.1 M KNO_3, using the linear region of a plot of mass change as a function of charge (Figure 13b). If it is assumed that during redox cycling one mole of redox site is converted, and electroneutrality is maintained strictly by the movement of cations present in the electrolyte, the apparent molar mass calculated should be 39 g/mol for PPy(PSS) in KNO_3. However, the value obtained for the apparent molar masses during the reductive process (M´r = -55.9) is higher than the molar mass of K, while the value obtained for the oxidative process (M´o = -39.6) was comparable to that obtained for this cation. This difference in mass observed for the reductive process is due to the movement of water molecules along with K^+ ions into the film. Solvent transfer has been shown to be an inherent feature of the charge compensation processes for hydrophilic polymers containing precisely defined redox sites [114]. It is also important to note the difference in value between M´r and M´o which could imply that not all species injected into the film during polymer reduction are ejected during its subsequent oxidation. For example, some water molecules may be retained in the film, resulting in a build-up of water in the polymer with further redox cycling. This hypothesis could also explain the drift in mass per cycle which is clearly seen when the film is subjected to multiple redox cycling and is described in Paper I.

The effect of subjecting the polymer film to multiple cycles of oxidation and reduction on the ion exchange behaviour is more evident quantitatively than qualitatively. With multiple cycling, the electroactivity of the films decreases slightly and structural/volume changes may also occur, which is accompanied by the accumulation of neutral species (water and salt). The latter is evident from the increase in mass with successive redox cycles after which the charge compensation mechanism becomes increasingly complex.

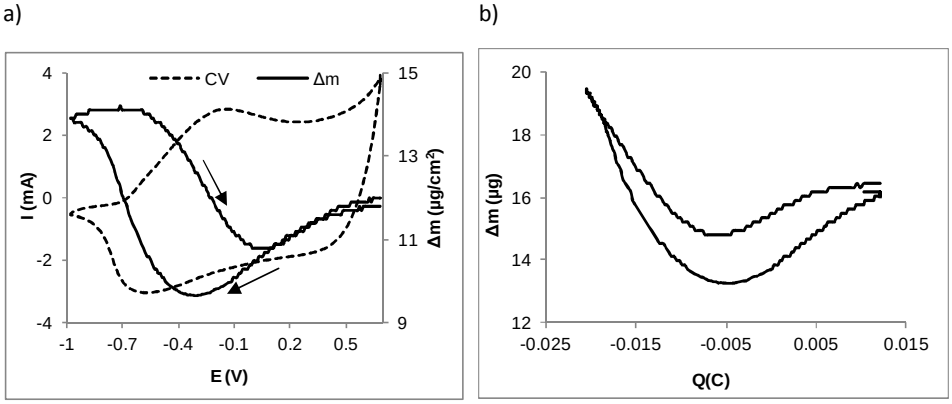

Figure 13: *(a) Scan 3 of a cyclic voltammetry experiment and mass changes accompanying reduction and oxidation of PPy(PSS) immersed in 0.1 M KNO_3 electrolyte. b) Mass change as a function of charge. The potential range was from +0.7 V to -1.0 V and scan rate was 100 mV/s (Paper I).*

A typical example of charge compensation being achieved through a combination of cation and anion exchange processes was observed when PPy(pTS) was immersed in 0.1 M KNO_3. Figure 14a shows the 3rd scan of the CV and accompanying mass changes for this system. During reduction of the film, a significant decrease in mass was observed, after which there was a slight increase in mass of the film. The decrease in mass is most likely due to the movement of anions out of the film, while the increase in mass is attributed to the movement of cations into the film. The net result of this combination of movement of anions and cations into and out of the film is that electroneutrality is maintained during the reduction process. On reversing the scan to the positive direction, an initial decrease in mass was observed followed by an increase in mass. The decrease in mass from 0.8V to 0 V is attributed to the release of cations that were incorporated during the reduction cycle, while the increase in mass observed when the potential was varied from -0.18 V to 0.6 V is attributed to the incorporation of anions from the surrounding media into the film. Thus, to maintain charge balance during the reduction and subsequent reoxidation of PPy(pTS) in KNO_3 there is

movement of nitrate ions in and out of the film at the more positive potentials, while K^+ ions move in and out of the film at the negative potentials [66, 115]. The CV in Figure 14a shows two reduction and two oxidation peaks, which also supports the conclusion that two different types of charge compensation processes are associated with the reduction and oxidation processes of PPy(pTS) in KNO_3 [76]. The reduction peak at ≈-0.95 V and oxidation peak at ≈-0.4 V correspond to the movement of K^+ into and out of the film, whereas the reduction peak at ≈ -0.1 V and oxidation peak at ≈ 0.2 V are associated with the corresponding movement of NO_3^- ions. The linear regions of a plot of mass change as a function of charge were used to determine the apparent molar mass of the ions involved in charge compensation during oxidation and reduction of PPy(pTS) immersed in 0.1 M KNO_3 for the 3rd CV scan (Figure 14b). For the reduction scan, M´ = 60.7 g/mol was calculated using data in the potential range from 0.55 V to -0.07 V. This value is not significantly less than the molar mass of nitrate (62 g/mol). A second M´ = -114.5 g/mol was calculated using data from the next linear range from -0.77 V to -0.93 V. During the oxidative scan, M´ = -60.8 g/mol was calculated from the first linear region between -0.76 V to 0.04 V, while the second M´ = -26.8 g/mol was calculated in the linear region between 0.22 V to 0.56 V. Each of these latter M´ values is not equivalent to either the molar mass of K^+ or NO_3^-. An explanation for this discrepancy is the movement of solvent molecules accompanying K^+ ions and the mo vement of water molecules in opposite direction to that of nitrate ions.

a) b)

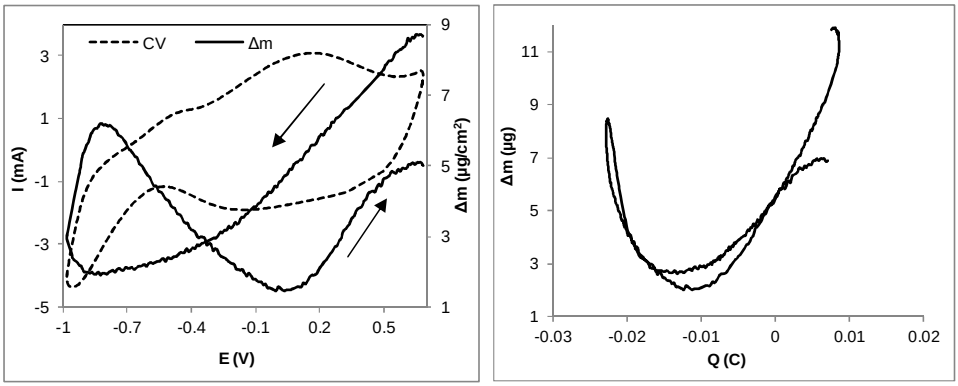

Figure 14: *(a) Scan 3 of a cyclic voltammetry experiment, and mass changes accompanying reduction and oxidation of PPy(pTS) immersed in 0.1 M KNO_3 electrolyte. (b) Mass change as a function of charge. The potential range was from +0.7 V to -1.0 V and the scan rate was 100 mV/s.*

The mixture of charge compensation processes observed for PPy(pTS) in KNO_3 is similar to that observed for PPy(C6S) immersed in KNO_3 . Figure 15a shows the 7th scan of the CV and accompanying mass changes for PPy(C6S) immersed in 0.1 M KNO_3. Linear regions of a plot of mass change as a function of charge (Figure 15b) were used to determine the apparent molar masses (M´) of the species/ions involved in charge compensation reactions for PPy(C6S) immersed in 0.1 M KNO_3. During reduction of the PPy(C6S) film within the potential range +0.6 V to -0.4 V, the apparent molar mass (M´) of the species causing the mass decrease was calculated to be -22.6 g/mol, which is much less than that of either nitrate or C6S. This suggests that simultaneous movement of anions and water molecules out of the film occurred, together with the movement of cations and water molecules into the film. On further reduction of the film below -0.4 V, the mass of the film increased due to incorporation of K^+ ions. The apparent molar mass of the species causing this mass increase was determined to be 42.3 g/mol which is slightly higher than that of K^+. During oxidation from -0.85 V to -0.2 V the mass of the film decreased again, which can be related to the movement of cations out of the film. PPy(C6S) films therefore demonstrate non-permselectivity with cations movement occurring in opposite direction to that of anions when cycled in KNO_3. To provide evidence that some C6S molecules remained in the polymer film even after multiple redox cycling events, EDXA was carried out on PPy(C6S) films before and after being subjected to 100 potential cycles (+0.6V to -0.85 V) in 0.1 M KNO_3. Emphasis was placed on sulphur in this study, since its presence in the polymer film can only be due to the presence of the dopant anion (C6S). A slight decrease in the content of sulfur in the PPy(C6S) film was observed after prolonged potential cycling in 0.1M KNO_3. In Paper III, EDXA results are presented which were obtained using PPy(pTS) film, which is a well known mixed ion exchanger. For this material, there was a decrease in sulphur content of about 50 % after the PPy(pTS) film had undergone a sustained period of consecutive reduction and oxidation reactions in 0.1 M KNO_3, which is consistent with mixed ion exchange behaviour. In contrast, the sulphur content before and after cycling the potential of a PPy(C6S) film immersed in $Mn(NO_3)_2$ remained almost unchanged (before cycling S = 0.15 % and after cycling S = 0.12%). This is consistent with the predominant cation exchange behaviour observed by EQCM experiments performed with PPy(C6S) in immersed in $Mn(NO_3)_2$ (Paper V). In spite of this small change in the content of sulfur after the PPy(C6S) film was subjected to 100 potential cycles, it can be assumed that the C6S

stayed inside the film at least in the beginning of the potential cycling procedure. Other studies have shown C6S anions to stay fixed inside the PPy film during doping reactions [116-118].

a) b)

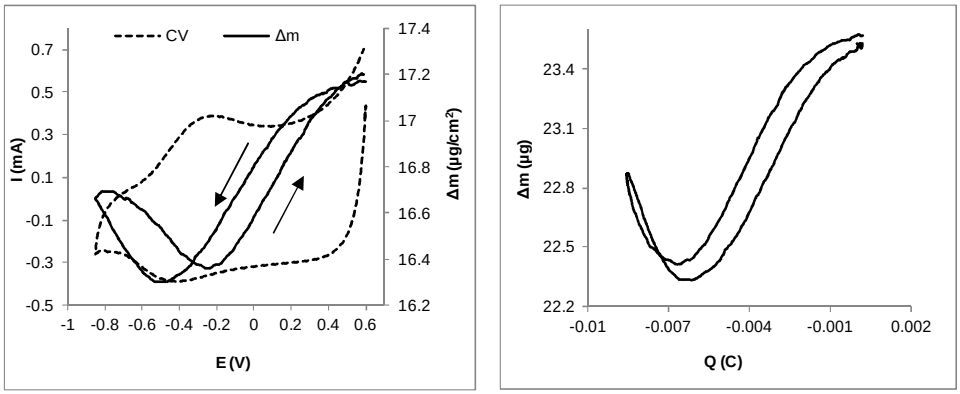

Figure 15: *(a) Scan 7 of a cyclic voltammetry experiment and mass changes accompanying reduction and oxidation of PPy(C6S) immersed in 0.1 M KNO_3 electrolyte. (b) Mass change as a function of charge. The potential range was from +0.6 V to -0.85 V and the scan rate was 100 mV/s (Paper V).*

A complex mixture of charge compensation processes was observed for PPy(CNT) films immersed in 0.1 M KNO_3. Figure 16a shows the 4th scan of the CV and accompanying mass changes for a PPy(CNT) film immersed in this electrolyte. The EQCM response is different from those exhibited by PPy films doped with immobile dopant anions such as that shown in Figure 13a for PPy(PSS), where exchange of cations is normally the dominant process. For the PPy(CNT) system, reducing the polymer by scanning the potential from +0.6 V to the negative direction initially led to a steep decrease in mass (Figure 16a), that is most likely due to the egress of nitrate ions from the polymer. Further reduction of the polymer subsequently led to a small increase in mass, which was attributed to the ingress of K^+ ions into the polymer. During the reverse scan, i.e. scanning from -0.85 V to the positive direction, no change in mass was observed until the potential was reached where the polymer was reoxidised. The steep increase in mass observed in this region is thought to be due to the movement of nitrate ions into the film to balance the positive charges created in the polymer backbone, which are not balanced by the carboxylated CNT anions. Charge compensation in PPy(CNT) films immersed in 0.1 M KNO_3, is therefore best summarised as occurring through a combination of mechanisms which involve movement of nitrate ions at more

positive potentials, and movement of cations at negative potentials. Evidence of both cation and anion exchange processes occurring was also obtained when EQCM experiments were performed using PPy(CNT) films immersed in 0.5 M KCl [119]. However, in the latter study charge compensation involved predominantly anion exchange reactions when the film was cycled in 0.5 M tetrabutylammonium bromide. This was attributed to the large size of the cation, which would be expected to inhibit its movement into and out of the polymer film.

Linear regions of a plot of mass change as a function of charge during redox cycling (4^{th} scan) of PPy(CNT) in 0.1 M KNO_3 (Figure 16b) were used to calculate the apparent molar masses (M´) of the species involved in the charge compensation reactions. A value for M´ of 212 g/mol was calculated using data obtained in the potential range where movement of nitrate ions into the film was the predominant mechanism of charge compensation. This value is considerably higher than the molar mass of the nitrate ion (62 g/mol), indicating that a significant number of water molecules (ca. 12 molecules of water) accompany the movement of nitrate ions during oxidation of the polymer. The value of M´ calculated from data obtained at negative potentials, where charge compensation was believed to be due primarily to the movement of K^+ ions was -151 g/mol. Therefore the movement of cations into the polymer film was also accompanied by the movement of a large number of water molecules. It is well known that redox cycling of PPy films results in the movement of ions and neutral species such as solvent molecules [120,121]. These processes are also responsible for the changes in volume of the film. The movement of this many water molecules makes it difficult to distinguish between the relative amounts of anion and cation movement, and their contributions to charge compensation, based solely on EQCM results. For example, while the larger changes in mass shown in Figure 16 are most readily accounted for by movement of anions, it is also possible that the results may be due to cation transfer processes occurring simultaneously with the movement of large number of water molecules in the opposite direction. The latter process would be expected to be facilitated by the very porous structure of PPy(CNT), observed by SEM, which would result in significant swelling and shrinking of the polymer film during redox cycling.

a) b)

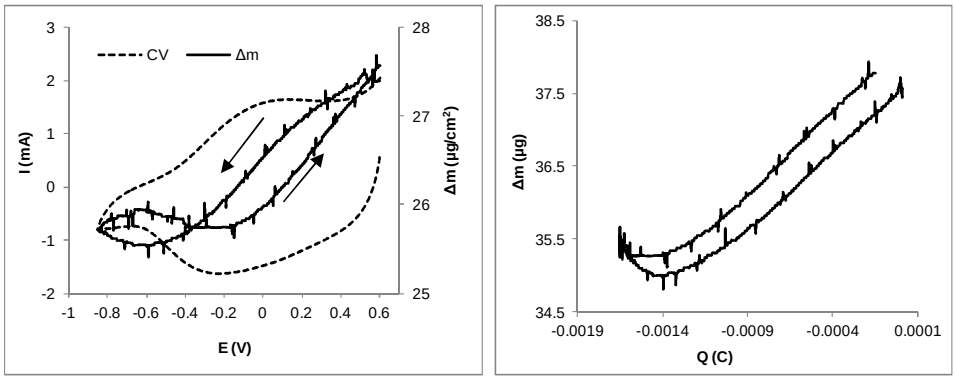

Figure 16: *(a) Scan 4 of a cyclic voltammetry experiment and mass changes accompanying reduction and oxidation of PPy(CNT) immersed in 0.1 M KNO_3 electrolyte. (b) mass change as a function of charge. The potential range was from +0.6 V to -0.85 V and scan rate was 100 mV/s (Paper IV).*

7.1.2. Surface Morphology and Film Thickness

SEM images of the surfaces and cross sections of PPy films used in transport studies were taken to investigate their surface morphologies and determine their film thicknesses. In addition, the morphology of PPy(C6S), PPy(pTS), PPy(PSS), PPy(CNT) and PPy(ClO_4) films before and after use in transport experiments were studied. Figure 17 shows SEM images of the surfaces of freshly prepared PPy films containing different dopant anions having different thicknesses. As can be seen in Figure 17, changing the dopant anion or the thickness of the polymer film has an effect on its morphology. For example, the typical cauliflower–like morphology characteristic of PPy films is evident in SEM micrographs of PPy(C6S), PPy(pTS) (2.7 μm thick film), and PPy(ClO_4) films shown in Figures 17a, b and f, respectively. However, Figure 17c shows that the surface of a 5.4 μm thick PPy(pTS) film consists of a dense, compact layer of material from which numerous spikes protrude. The PPy(PSS) film, on the other hand, has a highly dense and compact morphology (Figure 17d), but no protruding structures on its surface. In contrast to the above materials, the PPy(CNT) film shows a far more open and porous morphology consisting of intertwined fibres randomly deposited on the surface of the support material (Figure 17e). The porous nature of PPy(CNT) favours the movement of large amounts of water into and out of the film, accounting for the volume changes suggested by the results of the EQCM studies.

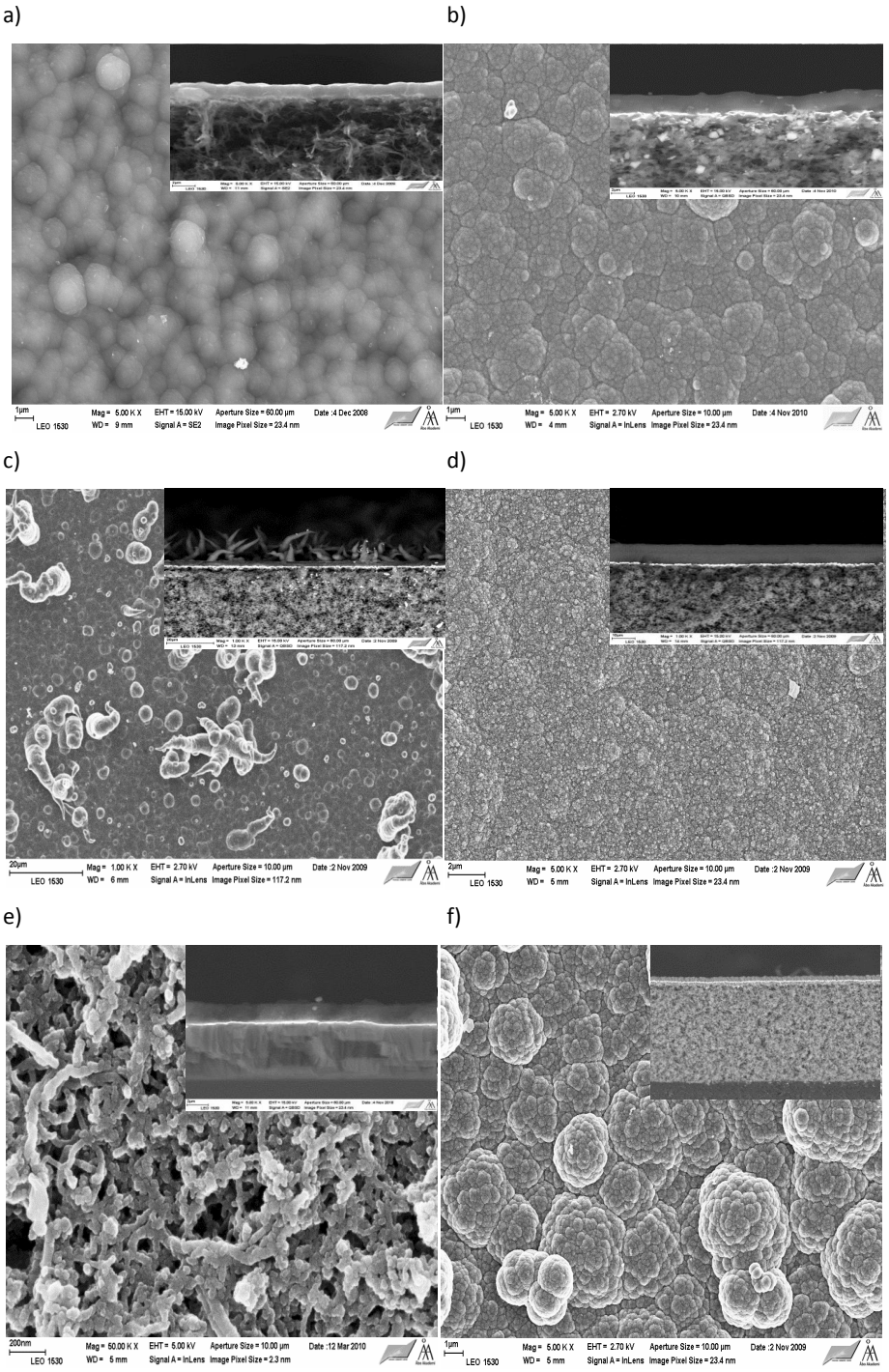

Figure 17: *SEM images of: (a) 1.8 µm thick PPy(C6S), (b) 2.7 µm thick PPy(pTS), (c) 5.4 µm thick PPy(pTS), (d) 10 µm thick PPy(PSS) and (e) 0.5 µm thick PPy(CNT) (f) 10 µm thick PPy(ClO_4). The inset on each micrograph shows a cross section of the same membrane (Papers II-IV).*

The cross sections of the PPy membranes shown as insets in Figure 17 were used to determine the thicknesses of the polymer films. A distinct layer of Pt can be seen in the cross section of the membranes containing PPy(pTS), PPy(PSS), PPy(CNT) as a bright line sandwiched between the PPy film and the support membranes. However, for the PPy(ClO_4) composite membrane, the Pt layer was sandwiched between two PPy layers, while for the PPy(C6S) composite membrane a distinct layer of Pt could not be observed between the support membrane and the PPy film. Table 3 compares the theoretical thicknesses of dry PPy films based on the charge consumed during polymerisation [122], with the experimental thicknesses determined by SEM. The theoretical thickness of the dry polymer film, *l*, was calculated according to Eq 7 [122].

$$l = \left(\frac{QM}{nFA\rho} \right) \qquad \text{Eq 7}$$

In this equation Q is the amount of charged passed during polymerisation, M is the molecular mass of the monomer, n = the number of electrons involved in the polymerisation and the degree of doping (the value for n was assumed to be 2.3, i.e. $2e^-$ per monomer unit and 0.3 e^- to dope the film to 30 %), A is the area of the electrode, F is the Faraday constant and ρ is the density of the film (approximated to 1g/cm^3).

There is good agreement between the calculated and measured thicknesses for the PPy(C6S), 2.7 µm thick PPy(pTS), PPy(PSS) and PPy(ClO_4) films but a large discrepancy exists between the calculated and measured thicknesses for the PPy(CNT) and 5.4 µm thick PPy(pTS) films. In the case of the former material, this could arise from the fact that PPy(CNT) films are highly porous, which would result in the measured thicknesses being higher than expected. Whereas the lower than expected thickness for the thicker PPy(pTS) film could be as a result of the formation of spikes on its surface. Furthermore, the method for calculating the thickness of the films assumes that they are of uniform density, which is not the case for the PPy(CNT) and 5.4 µm thick PPy(pTS) membranes.

Table 3: *Comparison of calculated and measured thicknesses of polypyrrole films.*

PPy film	Current density (mA/cm^2)	Time (min)	Calculated thickness (um)	Measured thickness (µm)
PPy(C6S)	1	10	1.8	2
PPy(C6S)	1	15	2.7	3.3
PPy(C6S)	1	30	5.4	5.6
PPy(pTS)	1	15	2.7	2.4
PPy(pTS)	1	30	5.4	2.8
PPy(PSS)	1	60	10.9	9.6
PPy(CNT)	0.05	60	0.54	2 - 7.9
PPy(ClO_4)	1	60	10.9	9.2

7.2. Influence of Dopant Anions on Metal Ion Flux

One of the main aims of this thesis was to study the effect of varying the dopant anion present in PPy membranes on their permeability towards divalent cations, e.g. Ca^{2+}, Mn^{2+} and Co^{2+}. For this reason, transport studies were carried out on PPy membranes prepared using C6S and CNT as dopant anions, as these were expected to produce differences in binding affinity for the divalent cations under investigation. This work is fully covered in Papers II and IV. The transport of ions across membranes based on PPy(PSS) and PPy(pTS) was also studied in order to understand the nature of ion transport and permeability across PPy(CNT) and PPy(C6S) membranes. Figure 18 shows the transport profiles of selected metal ions across: (a) PPy(C6S), (b)PPy(CNT), (c) PPy(pTS) and (d) PPy(PSS) composite membranes.

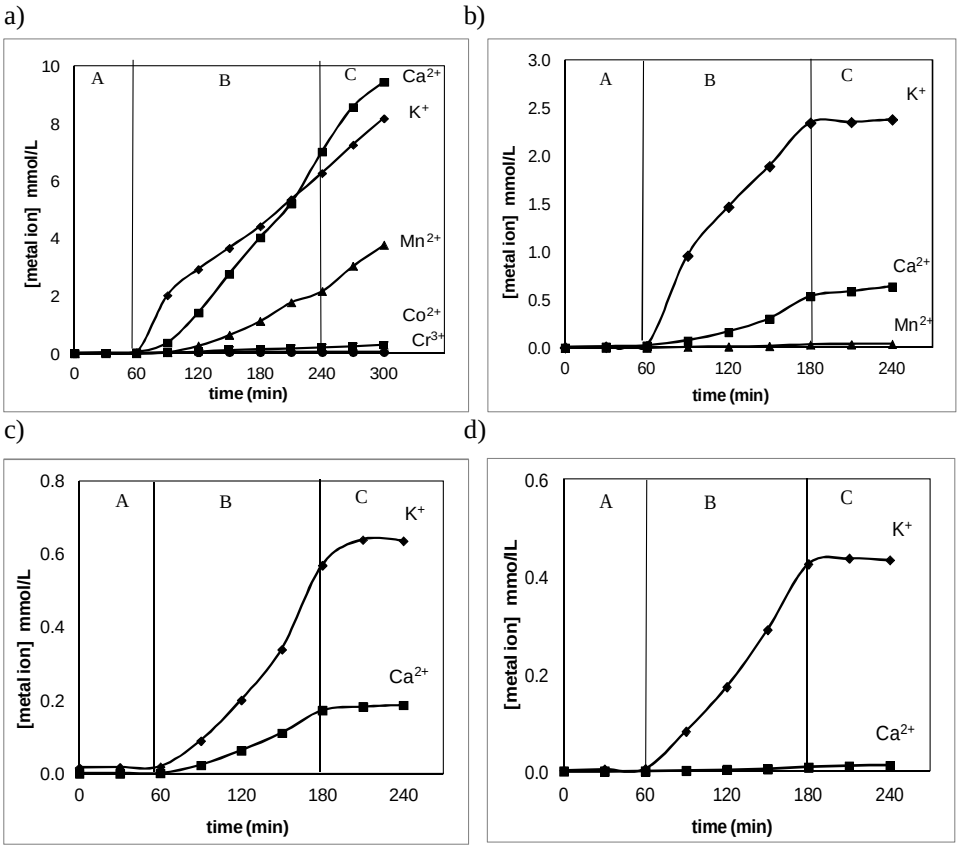

Figure 18: *Transport profiles for metal ions across PPy composite membranes containing different dopant anions; (a) PPy(C6S) on PVDF/Pt, (b) PPy(CNT) on PC/Pt, (c) PPy(pTS) on PVDF/Pt and (d) PPy(PSS) on PVDF/Pt. The source cell contained 0.1 M metal nitrate solution and the receiving cell contained deionised water. Region (A): no potential is applied, (B) pulsed potential waveform is applied (−0.8 V to +0.5 V, 50 s pulse width) and (C) no potential is applied. The transport studies were performed with solutions containing a single type of metal ion (Papers II-IV).*

The transport profiles shown in Figure 18 have three distinct phases A, B and C, depending on whether the membranes were subjected to pulsed potential wave form conditions (region B, or were left at open circuit potential (regions A and C). The transport profiles observed in Figure 18 show that when no potential was applied to the membrane there was no transport of metal ions (region A). However, in Region B, when a pulsed potential waveform was applied to the membrane, a significant flux of metal ions was observed. For most of the transport profiles in Figure 18, the transfer of metal ions from the source solution to the receiving solution ceased when the electrochemical stimulus was removed during the final phase of the experiment. This indicated that electrochemical control over the transport of metal ions across PPy(CNT), PPy(pTS)

and PPy(PSS) membranes was achieved. This was not the case, however, for the experiments performed with PPy(C6S) membranes. Figure 18a shows that in region A, when no potential was applied to the membrane, no metal ion transport occurred. However, in region B, when a pulsed potential was applied, metal ion transport was observed. In region C, when the applied potential was removed, the transport of K^+, Ca^{2+}, Mn^{2+}, and Co^{2+} across the membrane persisted. This situation had not previously been observed with PPy films prepared using other dopant anions. Once the PVDF/Pt-PPy(C6S) membrane had been electrochemically activated, metal ions continued to be transported from the source to the receiving solution even after the electrochemical stimulus was removed. One explanation that can be proposed to account for this behaviour is that microscopic holes had formed in the PPy(C6S) film during the period when the pulsed potential was applied. SEM images of a PVDF/Pt-PPy(C6S) film that had been subjected to electrical stimulation, however, did not show any evidence for the presence of microscopic holes. Furthermore, if such holes were routinely formed during region B of the transport experiments, then significant amounts of chromium should also have been detected in region C of the experiment performed with this metal ion. Another possible explanation for the unusual behaviour observed is that during region B there is an accumulation of metal ions in the membranes, which are slowly released even after the potential was removed. If this explanation is correct then the concentration of metal ions in the receiving solution of region C should not increase after a certain period of time. This hypothesis was investigated in a transport experiment performed using Ca^{2+} ions and a 3.3 μm thick PPy(C6S) film deposited on the PVDF/Pt substrate. A pulsed potential was applied to the membrane for only 30 minutes and the flux of Ca^{2+} ions was subsequently monitored for a further 24 hours. The results obtained showed that Ca^{2+} ions were continuously transported across the membrane once it had been electrochemically activated. At no point during the 24 hours of the experiment did the concentration of Ca^{2+} ions approach a limiting value. The driving force for this sustained ion flux was the concentration gradient between the source and the receiving solution. Eventually the concentration of Ca^{2+} ions in the receiving solution should reach a limiting value as this concentration gradient is reduced. A drawback associated with the PPy(C6S) membrane is therefore the inability to fully electrochemically control its metal ion permeability. It may still be possible to achieve electrochemical control over metal ion transport across PPy(C6S) membranes if other experimental conditions such as the support material that PPy film was deposited on had

been varied. However, this was not investigated for PPy(C6S) composite membranes in this thesis.

Figure 18a shows that K^+, Ca^{2+}, Co^{2+} and Mn^{2+} were transported across PPy(C6S) membrane to a significant extent during phase B of the experiment, while little or no transport of Cr^{3+}occured. Ca^{2+} and K^+ were transported most extensively, followed by Mn^{2+}, while the amount of Co^{2+} transported was significantly lower. At the end of the transport study with Co^{2+}, the whole surface of the membrane facing the receiving solution (when the receiving solution was deionised water) was covered with visible solid particles shown to be metallic cobalt by elemental analysis. No visible metal particles were found after the membranes had been in contact with Mn^{2+}, Ca^{2+} or K^+ ions. A similar set of metal ion transport profiles were observed using PPy(CNT) (Figure 18b), PPy(pTS) (Figure 18c) and PPy(PSS) (Figure 18d) membranes, with the exception that K^+ transport across the membrane was much higher than that of Ca^{2+} and Mn^{2+}. In fact the PPy(PSS) membrane proved to be impermeable towards Ca^{2+} ions. The lack of transport of Ca^{2+} across the PPy(PSS) film may be due to Ca^{2+} being trapped in the polymer as a result of ionic cross-linking during the reduction and oxidation processes. For example, PEDOT(PSS) was reported to be ionically cross-linked by multivalent cations [123]. In addition, it has been shown that a dispersion of PEDOT(PSS) precipitates when salts of divalent cations, e.g. Ca^{2+} and Mg^{2+}, are added [124]. Mangold et al. showed that there is a stronger Coulombic interaction between divalent cations and the fixed SO_3^- anions of PPy(PSS) films than there is with monovalent cations [125]. It should be noted that the flux of K^+ was also reported to be higher than that of Ca^{2+} in other previous metal ion transport studies involving PPy(PSS) composite membranes [86] or PPy(PSS) free-standing membranes [83]. The reason for the higher permeability towards K^+ was explained to be due to its smaller hydrated radius compared to that of Ca^{2+}.

Selectivity factor for K^+ over Ca^{2+} ($\propto_{Ca}^{K}$) was calculated for each PPy film (Table 4). The selectivity factor was calculated according to equation 8 (Eq 8) below.

$$\propto_{Ca}^{K} = \frac{flux\ of\ K^+}{flux\ of\ Ca^{2+}} \qquad \text{Eq 8}$$

Membrane Selectivity for K^+ over Ca^{2+} followed the order PPy(PSS) >> PPy(pTS) > PPy(CNT). For PPy(C6S) = 1.8 µm, the selectivity factor was close to 1, as can be seen

in Table 4. However when the thickness of PPy(C6S) was increased the selectivity factor was slightly increased. On the other hand, the selectivity factor for K^+ over Ca^{2+} for PPy(pTS) decreased from 14.1 to 3.4 with an increase in film thickness. Further experiments need to be performed in order to draw any definite conclusion regarding selectivity and polymer film thickness. The high selectivity of PPy(PSS) for K^+ was consistent when transport experiments were performed with single solutions of either K^+ or Ca^{2+} ion in the source cell as well as when the source solution contained a mixture of K^+ and Ca^{2+} ions in equal concentration. The high degree of selectivity for K^+ over Ca^{2+} showed by the PPy(PSS) membrane suggests that it may be suitable for performing metal ion separations on solutions containing both of these ions.

The calculated flux of the metal ions across the PPy membranes is presented in Table 4. The results show that the permeability of the PPy(C6S) membrane towards metal ions decreased according to the following sequence $Ca^{2+} \geq K^+ > Mn^{2+} >> Co^{2+}$, while the trend for PPy(CNT) was $K^+ >> Ca^{2+} > Mn^{2+}$, for PPy(pTS) it was $K^+ > Ca^{2+}$, and for PPy(PSS) it was $K^+ >> Ca^{2+}$. Most membranes showed much greater permeability towards K^+ than any other metal ion examined. The one exception to this general observation was PPy(C6S), which show an almost equal permeability towards K^+ and Ca^{2+}. In earlier studies, the permeability of the alkali metal and alkaline earth metal ions across composite membranes based on PPy doped with BCS [88], HQS [88] or CDS [89] was found to follow the order $K^+ \geq Na^+ > Ca^{2+} > Mg^{2+}$. This order was reported as being determined by variations in the size of the hydrated metal ions, with the smaller hydrated ions being able to pass more rapidly through pores present in the membranes [89]. It has also been shown previously that PPy(β-CDS) membranes are more permeable towards most metal ions than other types of PPy membranes such as PPy(α-CDS) [89], PPy(BCS) [88], PPy(HQS) [88] and PPy(PVS) [85]. For example, Reece et al. showed that PPy(β-CDS) membranes are about 10 times more permeable towards Mn^{2+}, Co^{2+}, Ni^{2+} and Zn^{2+} than those composed of PPy(HQS) or PPy(BCS) [89]. However, PPy(BCS) membranes showed higher permeability towards Fe^{3+} and Cu^{2+} than those consisting of PPy(β-CDS). The permeability of PPy(β-CDS) membranes towards alkali metal and alkaline earth metal ions was also reported to be considerably greater than that exhibited by most other previously studied PPy membranes [89]. However, the flux of Ca^{2+} ions across PPy(C6S) membranes reported here is higher than that observed for any other PPy membranes, including those doped with BCS, HQS or

β-CDS. It is also interesting to note that the permeability of PPy(CS6) membranes towards Mn^{2+} reported here is considerably higher than that observed with PPy(BCS) membranes, although it should be noted that in the current studies the receiving solution was deionised water, whereas for the study involving the latter membranes it was 0.1 M H_2SO_4. Surprisingly, PPy(HQS) membranes were reported to be completely impermeable towards Ca^{2+} and Mn^{2+} ions [88]. In contrast, the permeability of PPy(C6S) membranes towards Ca^{2+} reported here is the highest so far amongst PPy films doped with complexing ligands.

Table 4: *Comparison of permeability of PPy composite membranes towards selected metal ions.*

		Flux (x 10^{-8} mol/cm^2s)			
PPy Film	Film Thickness (μm)	K^+	Ca^{2+}	Mn^{2+}	α_{Ca}^{K}
PPy(C6S)	1.8	5.40	6.05	1.87	0.9
PPy(CNT) + DBS	2.2	9.32	2.50	0.15	3.7
PPy(pTS)	5.4	0.55	0.16		3.4
PPy(PSS) +DBS	10.9	0.38	0.01		36.4
PPy(C6S)	2.7	1.68	1.12		1.5
PPy(pTS)	2.7	5.84	0.41		14.1
*PPy(PSS) + DBS	10.9	0.42	0.01		41.8

** Transport study was performed with equimolar concentration of Ca and K solutions in the source cell.*

The permeability of metal ions across PPy membranes is influenced by a number of factors including the chemical nature of the ions, the size of the ions and the thickness of the PPy film. It can be seen from Table 4 that the metal ion permeability of the PPy membranes is significantly influenced by their thickness. For example, the flux of K^+ across 1.8 μm and 2.7 μm thick PPy(C6S) films were 5.4 x 10^{-8} mol/cm^2s and 1.68 x 10^{-8} mol/cm^2s, respectively. Similar results were obtained with PPy(pTS) membranes for which the permeability towards K^+ was 5.84 x 10^{-8} mol/cm^2s and 0.55 x 10^{-8} mol/cm^2s for 2.7 μm and 5.4 μm thick films, respectively.

7.3. The Effect of the Support Membrane on Transport of Metal Ions

In the pursuit to achieve electrochemical control over ion transport across membranes based on PPy, two main factors were considered. These were the type of support material upon which the PPy films were deposited, and also the effect of using either a monolayer or bilayer PPy film. Prior to the deposition of PPy on the support materials, a thin layer of platinum was deposited on their surfaces to make them electrically conducting. Figure 19 shows SEM micrographs of platinised PC and PVDF support membranes. The platinised PC membrane shows a number of uniform, cylindrical pores with precise diameters etched into its surface. In contrast, the surface of the platinised PVDF membrane shows an irregular network of pores with large variable openings. The average pore size of the PVDF membrane used in this study was 0.22 µm, while the pore size of the PC membrane was defined to be 0.1 µm. Figure 19 shows that the presence of a thin layer of platinum evenly distributed over the entire surface of the membranes did not result in any blockage of the surface pores.

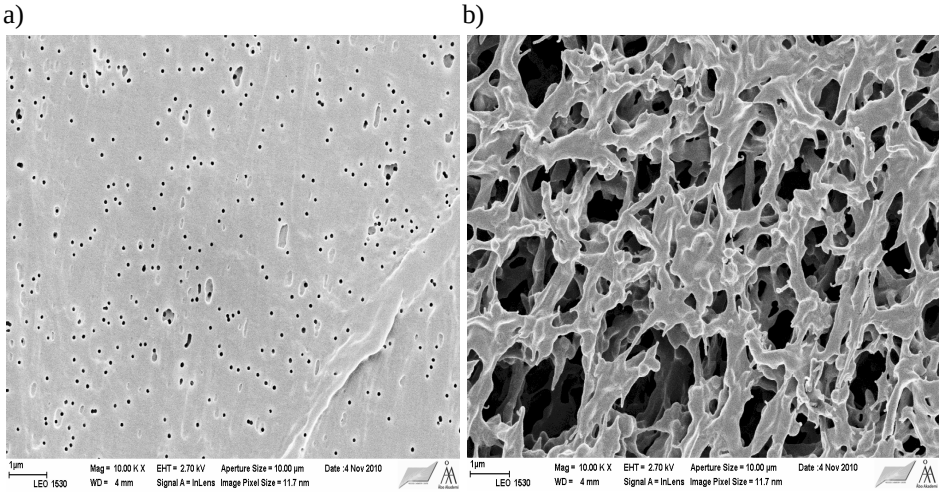

Figure 19: *SEM images of platinised support materials : (a) PC and (b) PVDF membranes (Paper IV).*

In order to investigate the influence of varying the support material on the permeability of the composite materials, studies were conducted with materials prepared by depositing PPy(CNT) and PPy(pTS) on PC and PVDF. Figure 20 shows the transport profile obtained for K^+ and membranes consisting of PPy(CNT) deposited on PVDF and PC. A continuous flux of K^+ across the membrane composed of PPy(CNT) deposited on

PVDF was observed, even before an electrochemical potential had been applied. Furthermore, the flux of K^+ ions was not significantly affected by applying a pulsed potential waveform during the second phase of the experiment, or by removing the applied potential. The flux of K^+ observed prior to application of the pulsed potential waveform is entirely attributable to the concentration gradient present across the membrane, and is perhaps not surprising in view of the highly porous surface morphology of this film revealed by SEM. In addition, the SEM image of the surface of a PPy(CNT) membrane (Figure 17e) shows that it has a morphology consisting of an irregular network of pores with larger diameter that can facilitate the movement of ions and solvent molecules. The above membrane morphology and permeability characteristics can be contrasted with that of a membrane produced by depositing PPy(pTS) on PVDF support material. The dense, compact PPy(pTS) film completely covers the pores of the underlying PVDF support material, thus preventing ion transport from occurring because of the concentration gradient between the source and receiving solutions.

a) b)

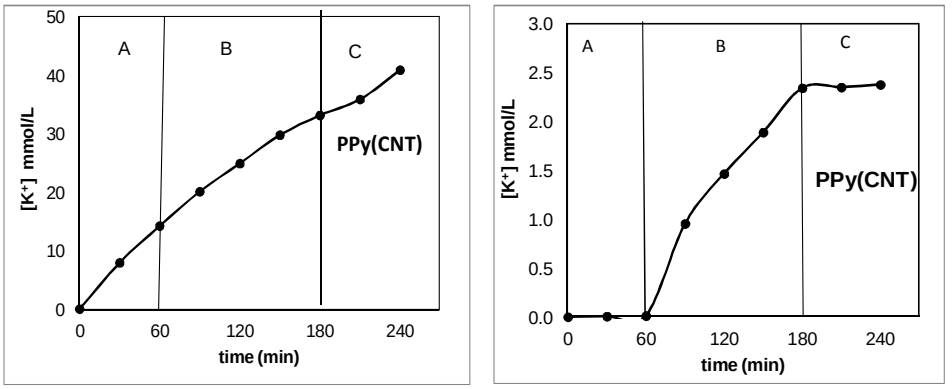

Figure 20: *Transport profiles for K^+ across PPy(CNT) deposited on: (a) PVDF and (b) PC. The source cell contained 0.1 M KNO_3 and the receiving cell contained deionised water. Region (A): no potential is applied, (B) pulsed potential waveform is applied (−0.8 V to +0.5 V, 50 s pulse width) and (C) no potential is applied (Paper IV).*

Membranes consisting of PPy(CNT) deposited on PC showed entirely different permeability characteristics compared to those prepared by depositing PPy(CNT) on PVDF. Figure 20b shows the transport profile obtained for the former membrane and potassium. The results obtained confirmed that ion transport across PPy(CNT) deposited on PC/Pt can be controlled electrochemically. In contrast, electrochemical

control over transport of K^+ across membranes composed of PPy(CNT) deposited on PVDF could not be achieved, even though the later materials were prepared under identical conditions. The highly uniform distribution of cylindrical pores with narrow openings in the PC support material contributes significantly to the ability to achieve electrochemical control over ion transport in the case of the composite membranes produced using this support material. In addition, in all cases where a direct comparison was possible, the flux of metal ions across composite membranes containing PC as the support material was slightly higher than for the same polymer film deposited on PVDF. This is probably because the PC support material is thinner (6 µm) than the PVDF membranes (100 µm) used.

The ability to exert electrochemical control over ion transport was also investigated using bilayer PPy films consisting of an initial layer of PPy(pTS) deposited on PVDF and a second layer of PPy(CNT). Figure 21 compares the transport profiles obtained for K^+ across the bilayer membrane and conventional PPy(pTS) films deposited on both PVDF and PC support membranes. The bilayer membrane was always oriented in the transport cell so that the PPy(pTS) layer was closer to the source solution. There was no transport of metal ions across the bilayer membrane or either across the PPy(pTS) membranes when no potential was applied. However, transport of K^+ ions did occur when a pulsed potential waveform was applied, and ceased when the electrochemical stimulus was removed. The flux of K^+ across the bilayer membrane was always higher than that across the conventional PPy(pTS) membrane. For example, the flux of K^+ across the PPy(pTS) membrane was 5.8×10^{-8} mol/cm^{2}s, whereas across the bilayer membrane it was 8.7×10^{-8} mol/cm^{2}s when the support material used was PVDF. This prompted the effect of changing the amount of PPy(CNT) present in the bilayer membrane on the flux of metal ion to be investigated. Doubling the thickness of the PPy(CNT) layer in the bilayer membrane resulted in the flux of K^+ increasing further to 12.4×10^{-8} mol/cm^{2}s. In general, it was observed that the flux of metal ions across membranes containing PPy(CNT) was higher than that across membranes containing PPy(pTS). One reason for this could be the increase in the bulk capacitance of the PPy layer when doped with CNT in combination with the more porous nature of PPy(CNT) film allowing fast transport of ions across such membranes.

a) b)

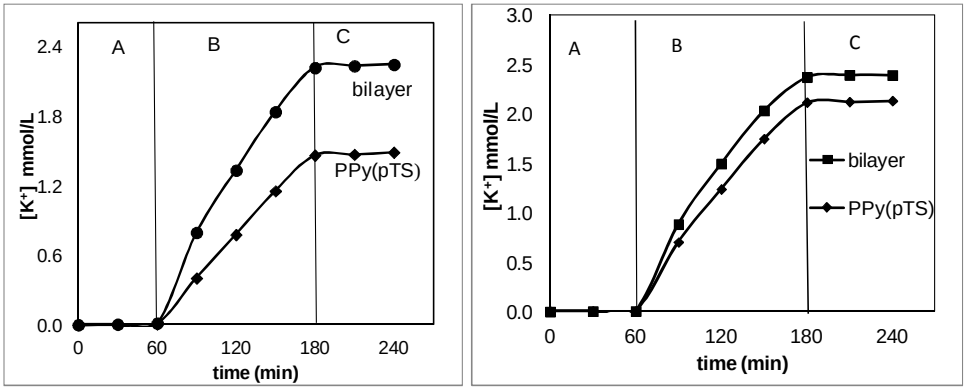

Figure 21: *Transport Profiles for K^+ across PPy films deposited on: (a) PVDF and (b) PC. The source cell contained 0.1 M KNO_3 and the receiving cell contained deionised water. Region (A): no potential is applied, (B) pulsed potential waveform is applied (−0.8 V to +0.5 V, 50 s pulse width) and (C) no potential is applied (Paper IV).*

7.4. Macroscopic Charge Compensation Mechanism

One of the main aims of this thesis was also to study the mechanism of macroscopic charge balance in the receiving solution during experiments in which anions or cations are transported across polypyrrole composite membranes. In order to study the mechanism, the concentrations of anions and cations in the receiving solution were monitored simultaneously in experiments performed using composite membranes which are known to have cation exchange (PPy(PSS)), anion exchange (PPy(ClO_4)) and mixed ion exchange properties (PPy(pTS)).

The concentration of K^+ and NO_3^- ions in the receiving solution of an experiment performed using a PPy(PSS) composite membrane is shown in Figure 22a. Both K^+ and NO_3^- ions permeated across the PPy(PSS) composite membrane, however, the flux of K^+ was about 3 times higher than that of NO_3^-. This is consistent with the results of EQCM studies presented in section 7.1.1, which showed that cation movement dominated the mechanism of charge compensation for PPy(PSS) immersed in aqueous KNO_3.

Figure 22b shows the transport profiles for Ca^{2+} and NO_3^- for an experiment performed using a PPy(ClO_4) composite membrane. It can be seen immediately that the transport of ions across a PPy(ClO_4) composite membrane could not be electrochemically

controlled. Even in region A, when no potential was applied, ions were transported across the membrane. In regions B and C, when a pulsed potential wave form (-0.8 V to 0.5 V, 50 s pulse width) was first applied to the membrane and then removed, ions continued to move across the membrane with approximately the same flux. The driving force for the transport of the ions across the membrane in this instance was the concentration gradient between the source and the receiving cell. Nonetheless, the flux of NO_3^- across the membrane is higher than that of Ca^{2+}. The dominant movement of anions (NO_3^-) across the PPy(ClO_4) membrane was expected since it is known to be a predominantly anion exchanging material owning to the small size of the dopant anion. The continuous leakage of ions across the membrane during the first phase of the experiment was probably due to the polymer film being not thick enough to stop the flux of anions while it was at open circuit potential. Attempts were not made to produce composite membranes containing thicker PPy(ClO_4) films because these would have greatly reduced the flux of the ions. Another possible explanation for the transport of calcium and nitrate ions in the absence of electrochemical stimulus is the open, porous morphology of the PPy(ClO_4) membrane revealed by SEM studies. Due to the porosity of the film, channels are created through which ions can flow even when the membrane is at open circuit potential.

Similar transport experiments to those described above were also performed with PPy(pTS) composite membranes. Figure 22c shows the transport profiles for K^+ and NO_3^- ions obtained in an experiment performed using a PPy(pTS) membrane. As can be seen in Figure 22c, anions and cations are transported across the PPy(pTS) membrane, indicating that it is not permselective. Furthermore, for every one mole of K^+ that was transferred across the membrane, one mole of NO_3^- was also transported. Similarly when the experiment was repeated using a source solution containing 0.1 M $Ca(NO_3)_2$, for every mole of Ca^{2+} that was transferred across the membrane, two moles of NO_3^- were transported. PPy(pTS) was shown to act as both a cation and anion exchanging material in the EQCM study presented in section 7.1.1, and EQCM studies of others [66,115].

a)

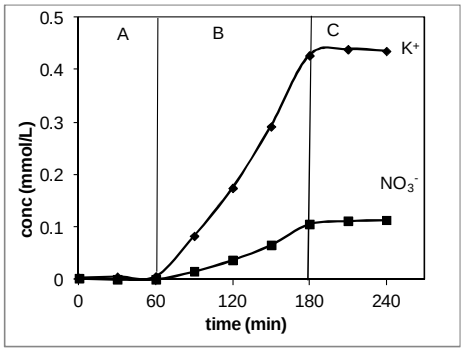

b)

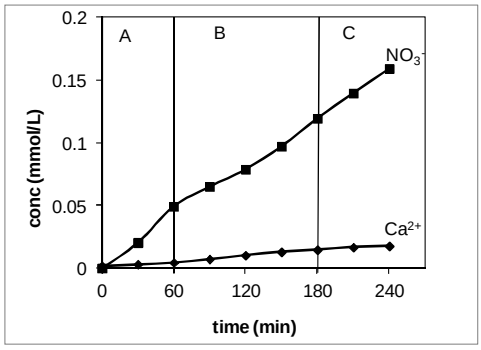

c)

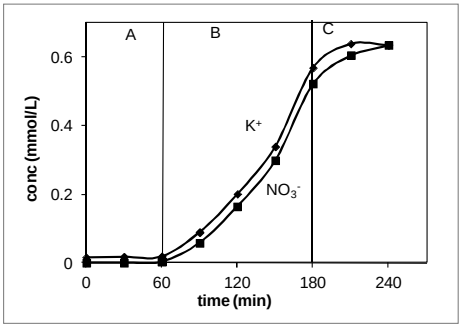

Figure 22: *Transport profiles for cations and anions across different composite membranes (a) PPy(PSS), (b) PPy(ClO_4) and (c) PPy(pTS). The source cell contained 0.1 M metal nitrate solution. Region A: no potential is applied, B) Pulsed potential waveform is applied (-0.8 V to +0.5 V, 50 s pulse width) and C) No potential is applied (Paper III).*

The results obtained from transport experiments and EQCM studies established that PPy(PSS), PPy(ClO_4) and PPy(pTS) films are not permselective. However, it was observed that the flux of cations is higher than that of anions across PPy(PSS) membranes, while the opposite was true for PPy(ClO_4) membranes. It is therefore important to understand how charge neutrality is maintained in the receiving solution when transport experiments are conducted with these membranes. In order to investigate this, the pH in the receiving solution was measured at the end of the transport experiments. Table 5 provides a summary of the measured pH values and the concentrations (mol/L) of ions in the receiving solution at the end of the transport experiments. Approximately equal amounts of K^+ and NO_3^- were transferred across the PPy(pTS) composite membrane, as the concentrations of these ions in the receiving solution at the end of the transport experiment were 6.4×10^{-4} mol/L and 6.3×10^{-4} mol/L, respectively. This indicates that for each mole of K^+ transported, about the same number

of moles of NO_3^- were transferred, resulting in charge balance being maintained in the receiving solution. In contrast, at the end of a transport experiment performed using an aqueous solution of KNO_3^- and a PPy(PSS) membrane, the receiving solution contained 4×10^{-4} mol/l K^+ and 1×10^{-4} mol/L NO_3^-. A third type of result was obtained from a transport experiment performed using a PPy(ClO_4) composite membrane and an aqueous solution of $Ca(NO_3)_2$ in the source cell. For this experiment, the concentration of NO_3^- (1.6×10^{-4} mol/L) in the receiving cell was higher than that of Ca^{2+} (1.2×10^{-5} mol/L). In both of the latter cases there was a surplus of either anions or cations from the source electrolyte in the receiving cell, which required additional counter ions to be transferred to or generated in the receiving solution in order to maintain overall charge balance.

The reaction that is most likely responsible for the production of these additional counter ions is the electrolysis of water. At 1.2 V vs. SHE, water is oxidised at the anode to produce protons (Reaction 10, R10), while at -0.83 V vs. SHE water is reduced at the cathode and hydroxide anions are produced (Reaction 11, R11) [122].

$$2H_2O \rightarrow O_2 + 4H^+ + 4e^- \qquad \text{R10}$$

$$2H_2O + 2e^- \rightarrow H_2 + 2OH^- \qquad \text{R11}$$

These reactions can produce either anions (OH^-) or cations (H^+) in the receiving solution, in order to maintain macroscopic electroneutrality. In the case of the experiments performed using a PPy(PSS) membrane and aqueous solution of KNO_3 in the source cell, the excess K^+ not compensated for by movement of NO_3^- ions during oxidation and reduction of the polymer, was most likely balanced by OH^- produced through the electrolysis of water. Since the electrochemical production of OH^- in the receiving solution would increase its pH, this hypothesis can be readily tested. The measured pH in the receiving solution after the transport experiment was 10.0 (Table 3), thus confirming the formation of an alkaline solution. In contrast, when a transport experiment was performed using a composite membrane containing PPy(ClO_4) and a source solution containing $Ca(NO_3)_2$, the final pH of the receiving solution was measured to be 4.8, which is distinctly acidic. Therefore, H^+ ions were produced in the receiving cell to compensate for the excess of anions transported during the course of the experiment. Table 5 also includes theoretical values for the pH of the solution in the

receiving cell at the end of the transport experiments. These calculated pH values were determined based on the assumption that the excess of cations (e.g. K^+ for the system involving PPy(PSS) and KNO_3) and anions (e.g. NO_3^- for the system involving PPy(ClO_4) and $Ca(NO_3)_2$) were compensated solely by the introduction of OH^- and H^+, respectively into the receiving cell. The calculated pH values are in good agreement with the measured pH.

Table 5: *pH and molar concentrations of cations and anions in the receiving solution at the end of transport experiment performed with PPy composite membranes (Paper III).*

Polymer	0.1 M source solution	[Metal ion] (mol/L)	[NO_3^-] (mol/L)	Measured pH	Calculated pH
PPy(PSS)	KNO_3	4×10^{-4}	1×10^{-4}	10.0	10.5
PPy(PSS)	$Ca(NO_3)_2$	-	-	6.6	
PPy(ClO_4)	KNO_3	4.4×10^{-5}	5.2×10^{-5}	6.0	
PPy(ClO_4)	$Ca(NO_3)_2$	1.2×10^{-5}	1.6×10^{-4}	4.8	3.9
PPy(pTS)	KNO_3	6.4×10^{-4}	6.3×10^{-4}	7.7	
PPy(pTS)	$Ca(NO_3)_2$	1.9×10^{-4}	3.4×10^{-4}	5.2	

8. Conclusion

The results of EQCM studies presented in this thesis demonstrated that the ion exchange behaviour of polypyrrole is dependent on a number of factors including the type of dopant anion present, the type of ions present in the surrounding medium, the scan rate used during the experiment and the previous history of the polymer film. When 0.1 M KNO_3 was used as the electrolyte and a scan rate of 100 mV/s was employed, charge compensation in PPy(PSS) films occurred principally through cation exchange, while for PPy(pTS), PPy(C6S) and PPy(CNT) it was achieved through a mixture of anion and cation exchange reactions.

The type of ions present in the surrounding electrolyte also greatly influenced the ion exchange behaviour exhibited by PPy films. For example, when PPy(PSS) films were used for EQCM experiments performed in 0.1 M $Al(NO_3)_3$ and $Cr(NO_3)_3$, charge compensation occurred principally by anion exchange reactions, contrary to the predominant cation exchange behaviour observed for experiments performed in aqueous KNO_3, $Ca(NO_3)_2$ and $Mn(NO_3)_2$ (Paper I). PPy(C6S) also exhibited charge compensation predominantly by cation exchange reactions when cycled in 0.1 M $Mn(NO_3)_2$, as opposed to the mixed ion exchange behaviour it showed when immersed in $Ca(NO_3)_2$ and KNO_3 solutions (Paper V).

A change in scan rate also influenced the ion exchange properties of PPy films to an extent. Qualitatively the EQCM results obtained using PPy(PSS) film immersed in 0.1 M KNO_3 were very similar when the scan rate was 20 mV/s or 100 mV/s. However, quantitative interpretation of the results obtained at 20 mV/s indicated that more complex ion exchange reactions were taking place with the amount of solvent moving in and out of the film clearly greater than at faster scan rates (Paper I).

The morphology of PPy films was found to change when the dopant anion was varied and even when the thickness of the film was altered in some cases. PPy(PSS) showed a uniform densely packed surface morphology, while the more typical cauliflower morphology was evident in PPy(ClO_4), PPy(C6S) and 2.7 µm thick PPy(pTS) films. Thicker films composed of PPy(pTS) showed an unusual morphology consisting of a dense, compact layer from which numerous spikes protrude. SEM imaging of

PPy(CNT), on the other hand, showed CNT coated with PPy to be randomly deposited on the surface of the support material, forming a porous, interconnecting three-dimensional network structure. The morphology of the films was also found to affect the mechanism of transport of ions across PPy membranes. Electrochemical control over transport of ions was easily achieved across composite membranes containing PPy(PSS) and PPy(pTS) films due to their compact morphology. In contrast, with composite membranes containing PPy(C6S) films it was not possible to exercise complete electrochemical control over ion transport. Electrochemical control over ion transport across PPy(CNT) composite membranes was obtained when films composed of the latter material were deposited on PC support material, whereas, the mechanism of ion transport was concentration gradient when the same film was deposited on PVDF. In addition, electrochemical control over ion transport was achieved using a composite membrane containing a PPy film consisting of PPy(pTS)/PPy(CNT), irrespective of the type of support material that was used in the transport experiments.

Transport of K^+, Ca^{2+}, Mn^{2+}, Co^{2+}, and Cr^{3+} across composite membranes containing PPy films doped with PSS, C6S, CNT and pTS was studied. The composite membranes consisted of PPy films deposited on commercially available membranes. Permeability of the membranes towards various metal ions did not show a significant dependence on the identity of the dopant anion. In nearly all cases the permeability of the membranes towards metal ions followed the order $K^+ > Ca^{2+} > Mn^{2+}$. The one exception was PPy(C6S) for which the permeability followed the order $Ca^+ \geq K > Mn^{2+} > Co^{2+} > Cr^{3+}$. The above permeability sequences show a strong dependence on the size of the metal ions with metal ions having the smallest hydrated radii exhibiting the highest flux. Another factor that affected the permeability towards metal ions was the thickness of the films, where the thinner films demonstrated higher metal ion fluxes. However, a composite membrane containing a bilayer film consisting of PPy(pTS)/PPy(CNT), with a total theoretical dry thickness of 3.3 μm showed a higher degree of permeability towards metal ions than a composite membrane containing a monolayer film of PPy(pTS) with a thickness of 2.7 μm. Therefore, the presence of CNT in the PPy film resulted in an increase in its permeability. Other factors such as the type of the support material used also affected the permeability of the composite membranes towards metal ions. In all cases where a direct comparison was possible, permeability of composite

membranes containing PC as the support material was slightly higher than for the same conducting polymer deposited on PVDF.

In the course of studying the mechanism of macroscopic charge balance in the receiving solution of a transport cell, it was established that PPy films were non permeslective. A clear correlation between the change in pH of the receiving solution and the type of ions transported across the membrane was observed. For example, a decrease in solution pH was observed when the polymer membrane achieved charge compensation primarily by acting as an anion exchange material, and an increase in pH was detected when the polymer functioned as a cation exchanger. When there was an approximately equal flux of anions and cations across the polymer membrane, the pH in the receiving solution was in the range 6 – 8. These observations suggest that macroscopic charge balance during the transport of cations and anions across polypyrrole membranes was maintained by the introduction of OH^- and H^+ produced via electrolysis of water in the receiving solution.

9. Remarks and Future Work

This thesis embodies fundamental work on the transport of cations across several examples of electroactive ion exchange membranes based on the conducting polymer polypyrrole. Since most PPy films are brittle as stand-alone membranes, the films were deposited on support materials to improve ease of handling. After considering the results presented here and elsewhere, it can be concluded that the dependence of the metal ion selectivity on the type of dopant ion present in the membrane is rather complex. However, the presence of a large dopant anion in the PPy film favoured transport of cations, while small dopant anions favoured transport of anions.

On the basis of EQCM studies alone, it was difficult to predict or establish the metal ion selectivity of the membranes. The selectivity of the membranes can be established by performing transport studies. The results obtained from an EQCM study performed using a PPy(C6S) film immersed in $Mn(NO_3)_2$ showed that this material acted predominantly as a cation exchanger, while a mixture of cation and anion exchange was observed when the electrolyte used was KNO_3 or $Ca(NO_3)_2$. Despite this, in transport experiments PPy(C6S) composite membrane was more permeable towards K^+ and Ca^{2+} than towards Mn^{2+}. Similarly, the results of an EQCM experiment that was performed using PPy(PSS) immersed in $Ca(NO_3)_2$ showed that this material achieved charge compensation predominantly by cation exchange reactions, while a transport experiment demonstrated that a composite membrane containing this film was impermeable towards Ca^{2+}. In order to understand these results, other characterisation tools should be used to study the ion exchange processes that occur during an actual transport experiment.

In this thesis, transport experiments were performed using several different types of ions including chiefly K^+ and Ca^{2+} but in some cases also Mn^{2+}, Co^{2+} and Cr^{3+}. The low permeability or non permeability of the membranes towards Co^{2+} and Cr^{3+}, and added complication of reduction of these metal ions during the electrochemical experiments prevented further examination of transport behaviour using these metal ions. In addition, transport experiments should be performed using source solutions containing a mixture of metal ions. This aspect was not fully explored in this thesis, and has not been fully

examined in other works on ion transport across PPy and/or other conducting polymer films.

EDXA was used in this thesis to study the mobility of the dopant anion when PPy films are reduced and then reoxidised. However, this could not be studied with PPy(CNT) films, since CNT contain carbon, hydrogen and oxygen (when carboxylated), which are also present in PPy or in the electrolyte studied. Thus, other methods such as X-ray photoelectron spectroscopy (XPS) should be used to monitor the dopant anion to establish its mobility in the PPy film during reduction and oxidation processes. The work described herein could also be extended to other types of conducting polymer films, e.g., PEDOT and their performance compared to that of the PPy membranes. It should also be noted that to date there are limited studies of the transport of anions across conducting polymer membranes with most work completed focused on metal ions. However, it is possible that conducting polymer membranes could be useful for the decontamination/separation of anions, especially those that do not precipitate easily.

In order to engender permselectivity the use of commercially available ion exchange membranes as the support material is suggested. Depositing PPy films on such membranes will also help in preventing fouling of the membrane. It will be worthwhile to compare the ion exchange performance of the membrane with and without a PPy film also present. Moreover, the transport experiments described herein should be scaled up to a prototype reactor in order to further investigate their potential for industrial use. Such membranes have high potential for separation processes, especially where conventional ion exchange membranes are currently used.

10. References

[1] P. K. Nagarale, G. S. Gohil, V. K. Sahi, R. Rangarajan. Colloids Surf. A. Physicochem Eng. Asp. 251 (2004) 133.

[2] P. K. Nagarale, G. S. Gohil, V. K. Sahi, G.S. Trivedi, R. Rangarajan. J. Colloid Interface Sci. 277 (2004) 162.

[3] T. Sata. J. Colloids Interface Sci. 44 (1973) 393.

[4] J. Benavente, A. Canas. J. Membr. Sci. 156 (1999) 241.

[5] E. Vallejo, G. Pourcelly, C. Gavach, R. Mercier, M. Pineri. J. Membr. Sci. 160 (1999) 127.

[6] T. Sata, R. Yamane, Y. Mizutani. J. Polym. Sci. Chem. Ed. 17 (1979) 2071.

[7] C. E. Harland. Ion Exchange Theory and Practice, 2nd Ed. Royal society of chemistry, Cambridge, 1994.

[8] M. Seko, H. Miyauchi, J. Omura in Ion Exchange Membranes. D. S. Flett (Ed), Ellis Horwood Limited, Chichester, West Sussex, England, 1983.

[9] P. G. Pickup, in Advanced Functional Molecules and Polymers. Electronic and Photonic Properties. H. S. Nalwa (Ed). Gordon and Breach Science Publishers, Amsterdam 2001, p 155.

[10] R. K. Nagarale, G.S. Gohil, V. K. Shahi. Adv. Colloid Interface Sci. 119 (2006) 97.

[11] T. Shimidzu, A. Ohtani, T. Iyoda and K. Honda. J. Electroanal. Chem. 224 (1987) 123.

[12] J. P. H. Sukamto, S. D. Rassat, R. J. Orth, M. A. Lilga. Water 1996 (2000) 2655.

[13] G. G. Wallace, G. M. Spinks, L. A. P. Kane-Maguire, P. R. Teasdale, Conductive Electroactive Polymers: Intelligent Materials Systems, 2nd Ed., CRC Press, Boca Raton, 2003.

[14] P. Burgmayer, R. W. Murray. J. Am. Chem. Soc. 104 (1982) 6139.

[15] M. Seno, M. Takagi, K. Takeda, M. Teramoto, T. Hashimoto (Eds.) Handbook of Separation Science, Kyoritsu Shuppan Co., Tokyo, Japan, 1993.

[16] H. Kawate, K. Tsuzura, H. Shimizu. Ion exchange membranes: in Ion Exchangers. K. Dorfner (Ed) Walter de Gruyter Berlin-New York, 1991.

[17] G. E. Molau. J. Membr. Sci. 8 (1981) 309.

[18] J. Bohziewicz, M. Bodzek, E. Wasik. Desalination 121 (1999) 139.

[19] M. Oldani, E. Killer, A. Miguel, G. Schook. J. Membr. Sci. 75 (1992) 265.

[20] Z. Amor. S. Malki, M. Taky, B. Bariou, N. Mameri, A. Elmidaoui. Desalination 120 (1998) 263.

[21] G. Saracco. Ann. Chmi. Rome 93 (2003) 817.

[22] E. Dejean, J. Sandeaux, R. sandeaux, C. Gavach. 33 (1998) 801.

[23] T. Xu. J. Membr. Sci. 263 (2005) 1.

[24] N. J. Bridger, C. P. Jones, M. D. Neville. J. Chem. Tech. Biotechnol. 50 (1991) 469.

[25] M. D. Neville, C. P. Jones, A. D. Turner. Progress in Nuclear Energy. 32 (1998) 397.

[26] I-H Loh, R. A. Moody. J. Membr. Sci. 50 (1990) 31.

[27] T. Ikeshoji. J. Electrochem. Soc 133 (1986) 2108.

[28] N. R. de Tacconi, K. Rajeshwar. Chem. Mater. 15 (2003) 3046.

[29] M. A. Lilga, R.J. Orth, J. P. H. Sukamto, S. M. Haight, D. T. Schwartz. Sep. Purif. Technol 11 (1997) 147.

[30] S. D. Rassat, J. H. Sukamto, R. J. Orth, M. A. Lilga, R. T. Hallen. Sep. Purif. Technol. 15 (1999) 207.

[31] K. M. Jeerage, D. T. Schwartz. Sep. Sci. Technol. 35, 15 (2000) 2375.

[32] M. A. Lilga, R. J. Orth, J. P. H. Sukamto, S. D. Rassat, J. D. Genders, R. Gopal. Sep. Purif. Technol. 24 (2001) 451.

[33] K. M: Jeerage, W. A. Steen, D. T. Schwartz. Chem. Mater. 14 (2002) 530.

[34] W. A. Steen, K. M. Jeerage, D. T. Schwartz. Appl. Spectrosc. 56, 8 (2002) 1021.

[35] J. Reyes-Gomez, J. A. Medina, K. M. Jeerage, W. A. Steen, D. T. Schwartz. J. Electrochem. Soc. 151 (2004) D 87.

[36] J. Bacskai, K. Martinusz, E. Czirok, G. Inzelt, P. Kulesza, M. A. Malik. J. Electroanal. Chem 358, 2, (1995) 241.

[37] J. A. Sukamto, S. D. Rassat, G. J. Josephson, W. E. Lawrence, D. p. Mendoza, V. V. Viswanathan, R. T. Hallen, R. J. Orth, M. A. Lilga, B. J. Malmberg, y. X. Gu, L.L. Edwards. Tappi J. 83, 6 (2000) 53.

[38] J. L. Brédas, G. B. Street. Polarons, Bipolarons and solitons in conducting polymers. Acc. Chem. Res. (1985) 309.

[39] W.R. Salaneck, R. H. Friend, J. L. Bredas. Phys. Rep. 319 (1999) 231.

[40] J. kankare in: electrical and optical polymer systems, fundamentals, methods, and applications, D. L. wise. G. E. Wnek, D. J. Trantolo, T. M. Cooper, J. D. Gresser (Eds.), Marcel Dekker, Inc., New York, 1998, 167.

[41] G. Inzelt. Conducting polymers in electrochemistry. F. Scholz (Eds). Springer-Verlag Berlin Heidelberg, 2008, 7.

[42] T. A. Skotheim, R. L. Elsenbaumer, J. R. Reynolds (Eds.), Handbook of Conducting Polymers, 2nd ed., Marcel Dekker, New York, 1998.

[43] G. Nyström, A. Razaq, M. Strømme, L. Nyholm, Nano Lett., 9 (2009) 3635.

[44] G. Nyström, M. Strømme, M. Sjödin, L. Nyholm, Electrochim. Acta 70 (2012) 91.

[45] H. Olsson, G. Nyström, M. Strømme, M. Sjödin, L. Nyholm, Electrochem. Commun. 13 (2011) 869.

[46] W.P. Su, J. R. Schrieffer, A. J. Heeger. Phys. Rev. Lett. 42 (1979) 1698.

[47] T. Ito, H. Shirakawa, S. Ikeda. J. Poly. Sci, Chem. Ed 12 (1974) 11.

[48] C. K. Chiang, Y. W. Park, A. J. Heeger, H. Shirakawa, E. J. Louis, A. G. Macdiarmid. J. Chem. Phys. 69 (1978) 5098.

[49] J. Heinze, B. A. Frontana-Ubribe, S. Ludwigs. Chem. Rev. 110 (2010) 4724.

[50] P. S. Tóth, E. Peintler-Kriván, C. Visy, Electrochem. Commun. 18 (2012) 16.

[51] C. Janáky, G. Cseh, P. S. Tóth, C. Visy, J. Solid State Electrochem. 14 (2010) 1967.

[52] A. J. Downard, D. Pletcher. J. Electroanal.Chem. 206 (1986) 147.

[53] S. Holdcroft, B. L. Flunt. J. Electroanal. Chem. 240 (1988) 89.

[54] W. Wernet, G. Wernet. Makromol. Chem. 188 (1987) 1465.

[55] S. Sadki, P. Schottland, N. Brodie and G. Sabouraud. Chem Soc. Rev. 29 (2000) 283.

[56] H. Eisazadeh, G. G. Wallace, G. Spinks. Polymer 35 (1994) 1754.

[57] J. Heinze. Electrochemistry of Conducting Polymers: in Organic Electrochemistry 4th Ed. H. Lund, O. Hammerich (Eds), Marcel Dekker, New York, USA, 2001.

[58] P. Pluger, M. Krounbi, G. B. Street. J. Chem. Phys. 78 (1983) 3212.

[59] J. M. Ribo, A. Dicko, M. A. Valles, J. Claret, P. Daliemer, N. Ferrer-Anglada, R. Bonnett, D. Bloor. Polymer 34 (1993) 1047.

[60] E. J. Oh, K. S. Jang. Synth. Met. 119 (2001) 109.

[61] J. Heinze. Synth. Met. 41-43 (1991) 2805.

[62] A. J. Heeger. Synth. Met. 125 (2002) 23.

[63] Z. Chen, A. Okimoto, T. Kiyonaga, T. Nagaoka. Anal. Chem., 71 (1999) 1834.

[64] N. Ogata. Macromol. Symp. 118 (1997) 693.

[65] P. S. Tóth, C. Janáky, O. Berkesi, T. Tamm, C. Visy, J. Phys. Chem. B 116 (2012) 5491.

[66] K. Naoi, M. Lien, W. H. Smyrl, J. Electrochem. Soc. 138 (2) (1991) 440.

[67] M. Lien, W.H. Smyrl, J. Electroanal. Chem. 309 (1991) 333.

[68] P. Burgmayer, R. W. Murray. J. Electroanal. Chem. 147 (1983) 339.

[69] P. Burgmayer, R. W. Murray. J. Phys. Chem. 88 (1984) 2515.

[70] T. Iyoda, A. Ohtani, T. Shimidzu, and K. Honda. Synth. Met. 18 (1987) 747.

[71] T. Shimidzu, A. Ohtani, and K. Honda. J. Electroanal. Chem. 251 (1988) 323.

[72] E. Wang, Y. Liu, S. Dong, J. Ding. J. Chem. Soc. Faraday Trans. 86 (12) (1990) 2243.

[73] E. Wang, Y. Liu, Z. Samec, C. Dvorak. Electroanalysis 2 (1990) 623.

[74] V. M. Schmidt, J. Heitbaum. Synth. Met. 31-43 (1991) 425.

[75] H. Zhao, W.E. Price, G.G. Wallace. J. Electroanal. Chem. 334 (1992) 111.

[76] H. Zhao, W.E. Price, C.O. Too, G.G. Wallace, D. Zhou. J. Membr. Sci. 119 (1996) 199.

[77] W. E. Price, C.O. Too, G.G. Wallace, D. Zhou. Synth. Met. 102 (1999) 1338.

[78] A. Mirmohseni, W.E. Price, C.O. Too, G.G. Wallace, H. Zhao. J. Int. Mater. Syst. Struct. 4 (1993) 43.

[79] H. Zhao, W. E. Price, G. G. Wallace. J. Membr. Sci. 87 (1994) 47.

[80] H. Zhao, W.E. Price, P.R. Teasdale, G.G. Wallace. React. Polym. 23 (1994) 213.

[81] D. Zhou, H. Zhao, W. E. Price, G. G. Wallace. J. Membr. Sci. 98 (1995) 173.

[82] A.C. Partridge. Electrochim. Acta 40 (1995) 1199.

[83] A.C. Partridge, C. Milestone, C.O. Too, G.G. Wallace. J. Membr. Sci. 152 (1999) 61.

[84] H. Zhao, W. E. Price, G. G. Wallace, Polymer 34 (1) (1993) 16.

[85] J. M. Davey, S. F. Ralph, C. O. Too, G. G. Wallace, Synth. Met. 99 (1999) 191.

[86] J. M. Davey, S. F. Ralph, C. O. Too, G. G. Wallace, A. C. Partidge. React. Funct. Polym. 49 (2001) 87.

[87] A. Mirmohseni, W. E. Price, G. G. Wallace. J. Membr. Sci. 100 (1995) 239.

[88] V. Misoska, J. Ding, J. M. Davey, W. E. Price, S. F. Ralph, G. G. Wallace. Polymer 42 (2001) 8571.

[89] D.A. Reece, S.F. Ralph, G.G. Wallace. J. Membr. Sci. 249 (2005) 9.

[90] J. Ding, W. E. Price, S. Ralph, G. GWallace. Synth. Met. 119 (2001) 357.

[91] C. Ehrenbeck, K. Jüttner. Electrochim. Acta 41 (1996) 511.

[92] C. Ehrenbeck, K. Jüttner. Electrochim. Acta 41 (1996) 1815.

[93] G. S. Gohil, V. V. Binsu, V. K. Shahi. J. Membr. Sci. 280 (2006) 210.

[94] M. J. Ariza, T. F. Otero. J. Membr. Sci. 290 (2007) 241.

[95] M. J. Ariza, T. F. Otero. Colloids and Surfaces A: Physiochem. Eng. Aspects 270-271 (2005) 226.

[96] A. C. Partridge, C. Milestone, C. O. Too, G. G. Wallace. J. Membr. Sci. 132 (1997) 245.

[97] M. R. Deakin, D. A. Buttry. Anal. Chem. 61 (1989) 1147A.

[98] D. A. Buttry, Electroanal. Chem. (A.J. Bard, ed.) Dekker, New York, 1991 vol 17, p. 1.

[99] D. Buttry, M. D. Ward, Chem. Rev. 92 (1992) 1355.

[100] M. D. Ward, Phys. Electrochem. (I. Rubinstein, ed.) Deker, New York, 1995, p. 293.

[101] A. W. Bott, Current Separations 18:3 (1999) 79.

[102] C. Lu, A. W. Czanderna (Eds), Applications of the Piezoelectric Quartz Crystal Microbalance (Methods and Phenomena Series), 7 (1984) New York: Elsevier.

[103] D. Buttry, The Quartz crystal Microbalance as an In-situ Tool in Electrochemistry in Electrochemical Interfaces: Modern techniques for In-situ Interface Characterization H. D. Abruňa (Ed.) VCH Publishers, Inc , New York, p. 531, 1991.

[104] C. Debiemme-Chouvy, A. Rubin, H. Perrot, C. Deslouis, H. Cachet. Electrochim. Acta 53 (2008) 3836.

[105] C. Baker, J. Reynolds, J. Electroanal. Chem. 245 (1988) 307.

[106] C. Weidlich, K.-M. Mangold, K. Juttner, Electrochim. Acta 50 (2005) 1547-1552.

[107] D. A. Skoog, J. J. Leary. Principles of Instrumental Analysis, 4th Ed., Saunders College Publishing, 1992.

[108] H. H. Willard, L. Merritt, J. A. Dean, F. A. Settle. Instrumental Methods of Analysis, 7th Ed., Wadsworth Publishing Company, California, p 287, 1988.

[109] C. B. Boss, K. J. Fredeen. Concepts, Instrumentation and Techniques in Inductivley Coupled Plasma Optical Emission Spectrometry. 3rd ed. PerkinElmer, Inc, USA, 2004.

[110] G. H. Jeffrey, J. Bassett, J. Mendham, R. C. Denney. Vogel's Textbook of Quantitative Chemical Analysis. 5th ed. Longman Group U K Limited, 1989.

[111] J. Janata, Principles of Chemical Sensors, Springer, New York, 2009.

[112] J. Bobacka, A. Ivaska, in Electropolymerization (Eds: S. Cosnier, A. A. Karyakin), Wiley-VCH, 2010.

[113] C. Weidlich, K.-M. Mangold, K. Juttner,. Electrochim. Acta 50 (2005) 1547.

[114] S. Bruckenstein and A.R. Hillman, J. Phys. Chem. 92 (1988) 4837.

[115] V. Syritski, A. Öpik, O. Forsén. Electrochim. Acta 48 (2003) 1409.

[116] G. Bidan, M.-A. Niel, Synth. Met. 85 (1997) 1387.

[117] Z. Mousavi, J. Bobacka, A. Ivaska, Electroanal. 17 (2005) 1609.

[118] D. A. Reece, J. M. Pringle, S. F. Ralph, G.G. Wallace, Macromol. 38 (2005) 1616.

[119] G. A. Snook, G. Z. Chen, D. J. Fray, M. Hughes, M. Shaffer. J. Electroanal. Chem. 568 (2004) 135.

[120] S. Bruckenstein, J. Chen, I. Jureviciute, A. R. Hillman. Electrochim. Acta 54 (2009) 3516.

[121] T.F. Otero, J. Padilla.J. Electroanal. Chem. 561 (2004) 167.

[122] A. J. Bard, L. R. Faulkner. Electrochemical Methods: Fundamentals and Applications. 2nd Ed., John Wiley & Sons, Inc, New York, 2001.

[123] M. Vázquez, P. Danielsson, J. Bobacka, A. Lewenstam, A. Ivaska, Sens. Actuators, B 97 (2004) 182.

[124] S. Ghosh, O. Inganäs. Synth. Met. 101 (1999) 413.

[125] K.-M. Mangold, C. Weidlich, J. Schuster and K. Juttner. J. Appl. Electrochem. 35 (2005) 1293.

ÅBO AKADEMI
UNIVERSITY

ISBN 978-952-12-2820-9

Painosalama Oy - Turku, Finland 2012